



## RESEARCH ARTICLE

# Ecophysiological analysis reveals distinct environmental preferences in closely related Baltic Sea picocyanobacteria

Anabella Aguilera<sup>1</sup>  | Javier Alegria Zufia<sup>1</sup> | Laura Bas Conn<sup>1</sup> |  
Leandra Gurli<sup>1</sup> | Sylwia Śliwińska-Wilczewska<sup>2,3</sup> | Gracjana Budzałek<sup>3</sup> |  
Daniel Lundin<sup>1</sup>  | Jarone Pinhassi<sup>1</sup> | Catherine Legrand<sup>1,4</sup> | Hanna Farnelid<sup>1</sup>

<sup>1</sup>Department of Biology and Environmental Science, Centre for Ecology and Evolution in Microbial Model Systems (EEMiS), Linnaeus University, Kalmar, Sweden

<sup>2</sup>Mount Allison University, Sackville, New Brunswick, Canada

<sup>3</sup>Laboratory of Marine Plant Ecophysiology, Institute of Oceanography, University of Gdansk, Gdynia, Poland

<sup>4</sup>School of Business, Innovation and Sustainability, Halmstad University, Halmstad, Sweden

## Correspondence

Anabella Aguilera, Department of Biology and Environmental Science, Centre for Ecology and Evolution in Microbial Model Systems (EEMiS), Linnaeus University, Kalmar, Sweden.  
Email: [anabella.aguilera@lnu.se](mailto:anabella.aguilera@lnu.se)

## Funding information

Anna-Greta and Holger Crafoord Foundation, Grant/Award Number: CR2019-0012; Knut och Alice Wallenbergs Stiftelse, Grant/Award Number: 570630-3095; Svenska Forskningsrådet Formas, Grant/Award Number: 2017-00468; Strategic Research Programme Ecochange; Canada Foundation for Innovation; New Brunswick Innovation Foundation

## Abstract

Cluster 5 picocyanobacteria significantly contribute to primary productivity in aquatic ecosystems. Estuarine populations are highly diverse and consist of many co-occurring strains, but their physiology remains largely understudied. In this study, we characterized 17 novel estuarine picocyanobacterial strains. Phylogenetic analysis of the 16S rRNA and pigment genes (*cpcB* and *cpeBA*) uncovered multiple estuarine and freshwater-related clusters and pigment types. Assays with five representative strains (three phycocyanin rich and two phycoerythrin rich) under temperature (10–30°C), light (10–190  $\mu\text{mol photons m}^{-2} \text{s}^{-1}$ ), and salinity (2–14 PSU) gradients revealed distinct growth optima and tolerance, indicating that genetic variability was accompanied by physiological diversity. Adaptability to environmental conditions was associated with differential pigment content and photosynthetic performance. Amplicon sequence variants at a coastal and an offshore station linked population dynamics with phylogenetic clusters, supporting that strains isolated in this study represent key ecotypes within the Baltic Sea picocyanobacterial community. The functional diversity found within strains with the same pigment type suggests that understanding estuarine picocyanobacterial ecology requires analysis beyond the phycocyanin and phycoerythrin divide. This new knowledge of the environmental preferences in estuarine picocyanobacteria is important for understanding and evaluating productivity in current and future ecosystems.

## INTRODUCTION

The picocyanobacterium *Synechococcus* is a significant primary producer with a cosmopolitan distribution in marine, estuarine, and freshwater ecosystems (Callieri et al., 2013; Partensky et al., 1999; Visintini et al., 2021). Organisms classified as *Synechococcus* are polyphyletic (Honda et al., 1999; Salazar et al., 2020), but the majority of the representatives have been taxonomically placed into a cyanobacterial lineage termed cluster 5 (Castenholz, 2001). Cluster

5 encompasses a separate branch comprising the genus *Prochlorococcus* and three major lineages, called sub-clusters 5.1, 5.2, and 5.3 (Ahlgren & Roco, 2012). Sub-cluster 5.1 is mainly composed of pelagic marine strains and it is the most widespread lineage in the open ocean environment (Farrant et al., 2016). Extensive work combining global field observations, metagenomics, and physiological work with isolates has revealed a high genetic and functional diversity within this sub-cluster and multiple genetic lineages (clades) have been identified (Doré et al., 2020;

This is an open access article under the terms of the [Creative Commons Attribution](https://creativecommons.org/licenses/by/4.0/) License, which permits use, distribution and reproduction in any medium, provided the original work is properly cited.

© 2023 The Authors. *Environmental Microbiology* published by Applied Microbiology International and John Wiley & Sons Ltd.

Farrant et al., 2016; Ferrieux et al., 2022; Mackey et al., 2017; Pittera et al., 2014; Six et al., 2021; Sohm et al., 2016). These lineages are physiologically specialized in different niches, revealing the existence of ecotypes defined by environmental factors such as temperature and light. Sub-cluster 5.3 includes both open ocean strains and a cosmopolitan group of freshwater strains (Cabello-Yeves et al., 2017, 2018; Scanlan et al., 2009). Finally, the genetically diverse sub-cluster 5.2 spans a wide range of salinity adaptations containing freshwater, brackish, and halotolerant strains (Cabello-Yeves et al., 2018; Cabello-Yeves, Callieri, et al., 2022; Cabello-Yeves, Scanlan, et al., 2022; Callieri et al., 2021, 2022; Di Cesare et al., 2018; Sánchez-Baracaldo et al., 2019) and contains a mix of strains assigned to *Cyanobium* spp. and *Synechococcus* spp. Compared to the marine pelagic water counterpart, knowledge about the ecological role of *Synechococcus* in dynamic coastal and estuarine ecosystems is limited and the physiological characteristics and relationships among lineages and clades within sub-cluster 5.2 remain largely indeterminate (Callieri et al., 2013, 2022). Comparative genomics has brought novel insights into the genetic diversity of *Synechococcus*, and as a consequence, the taxonomy of the genus is under revision and deep transformation. While recently updated comparative genomic studies that used average nucleotide/amino acid identity (AAI/ANI) values proposed to split *Synechococcus* into three distinct taxa: *Ca. Marinosynechococcus* (sub-cluster 5.2), *Cyanobium* (all strains assigned to sub-cluster 5.2), and *Ca. Juxtasynechococcus* (sub-cluster 5.3) (Doré et al., 2020), other studies based on genome-level analyses proposed to split *Synechococcus* into 15 separated genera (Salazar et al., 2020).

The contribution of *Synechococcus* to primary production and phytoplankton biomass in estuaries is significant (Alegria Zufia et al., 2021; Bertos-Fortis et al., 2016; Paerl et al., 2020; Xia et al., 2015). Estuarine systems sustain *Synechococcus* populations consisting of diverse co-occurring strains, which are not yet phylogenetically well defined (Celepli et al., 2017; Chen et al., 2006; Haverkamp et al., 2009; Xu et al., 2015). Moreover, few estuarine strains have been physiologically characterized or genome sequenced (Cabello-Yeves, Callieri, et al., 2022; Cabello-Yeves, Scanlan, et al., 2022; Fucich et al., 2021; Marsan et al., 2014; Śliwińska-Wilczewska et al., 2018; Xu et al., 2015). The lack of representative estuarine strains and physiological studies limits the assessment of *Synechococcus* ecotypes and their role in these ecosystems (Callieri, 2017; Callieri et al., 2022).

*Synechococcus* display a unique diversity of photosynthetic pigments, which extends the light niches that this picocyanobacterium can occupy. Thereby, pigment composition is considered an important determinant of *Synechococcus* distribution. Besides chlorophyll *a* (Chl

*a*), mainly associated with photosystem I, *Synechococcus* contain phycobilisomes (PBS), which funnel light energy to photosystem II (Scanlan et al., 2009; Six et al., 2007). PBSs are composed of a core of allophycocyanin and rods of variable phycobiliprotein composition (Six et al., 2007). Based on the composition of the phycobiliproteins, *Synechococcus* strains are divided into three main pigment types: pigment Type I containing only phycocyanin (PC, encoded by the *cpcBA* operon), pigment Type II containing PC and one form of phycoerythrin (PE-I, encoded by *cpeBA*), and pigment Type III containing PC and two forms of PE (PE-I and PE-II, encoded by *cpeBA* and *mpeBA*, respectively). While pigment Type I strains (PC-rich) are green and pigment type II (PE-rich) red, pigment Type III presents a wide range of pigmentation, and some display chromatic adaptation (Scanlan et al., 2009; Six et al., 2007). While pigment Type III dominates in open marine environments where blue light prevails, pigment Types I and II are mostly found in coastal waters, estuaries, and freshwater systems (Cabello-Yeves et al., 2017; Grébert et al., 2018; Larsson et al., 2014; Stomp et al., 2007). A metagenomic study identified a novel pigment cluster, Type IIB, as being dominant in the brackish waters of the Baltic Sea (Larsson et al., 2014). Type IIB was also recently identified in whole-genome sequenced picocyanobacterial strains isolated from freshwater lakes (e.g. *Cyanobium usitatum* Tous, *Synechococcus* sp. 8F6, *Synechococcus* sp. 1G10, *Vulcanococcus limneticus* LL; Cabello-Yeves et al., 2018; Sánchez-Baracaldo et al., 2019) but appears to be absent in major oceanic basins (Grébert et al., 2018). The eco-physiology of Type IIB strains and the potential links to their distribution remains unexplored.

Typically, PC-rich cells (pigment Type I) predominate in high turbid waters where red light prevails, such as low salinity surface waters, estuaries, and eutrophic lakes (Paerl et al., 2020; Wang et al., 2011). PE-rich strains of pigment Type II are considered to be adapted to blue and green light absorption and tend to be more abundant in low-turbidity waters such as the transition zones between brackish and marine environments, and deep, clear lakes (Callieri & Stockner, 2002; Larsson et al., 2014). In waters of intermediate turbidity like coastal waters, estuaries, and freshwater lakes, the physiological diversity of *Synechococcus* is high and multiple pigment types co-occur (Haverkamp et al., 2008, 2009; Larsson et al., 2014; Liu et al., 2014; Stomp et al., 2007; Wang et al., 2011; Xia et al., 2017). Thus, other factors apart from light may have a key role in their niche differentiation. For example, environmental factors like nutrients, salinity, and temperature directly affect the distribution and seasonality of co-occurring strains in estuarine systems (Alegria Zufia et al., 2021; Jiang et al., 2016; Paerl et al., 2020; Wang et al., 2011). In addition, large differences in growth

have been observed in experiments with estuarine *Synechococcus* strains using broad temperature, salinity, and light gradients (Śliwińska-Wilczewska et al., 2018, 2020). This suggests high physiological plasticity in relation to changing environmental conditions in estuarine *Synechococcus*, but the links between physiological studies and environmental dynamics are not yet well established.

In this study, we characterized 17 novel strains of cluster 5 picocyanobacteria isolated from the Baltic Sea. Picocyanobacteria are important contributors to phytoplankton biomass in this large estuarine ecosystem (up to ~80% in summer), and high-throughput sequencing has revealed a large diversity and seasonal shifts of picocyanobacterial strains (Alegria Zufia et al., 2021, 2022; Bertos-Fortis et al., 2016; Celepli et al., 2017; Larsson et al., 2014). The strains were identified using flow cytometry, microscopy, and amplification and sequencing of fragments of the 16S rRNA, *cpcB*, *cpeBA*, and *mpeBA* genes. The amplicon sequence variants (ASVs) of the 16S rRNA gene were identified in amplicon sequence libraries from a coastal and an offshore monitoring station to identify the contribution to the picocyanobacterial community and the seasonal in situ dynamics. In addition, based on the phylogenetic affiliation and seasonality of ASVs, five strains were chosen for further characterization of their pigmentation and physiology. Our results bring insights into the diversity and ecophysiology of unexplored estuarine picocyanobacteria and their environmental niche preferences.

## EXPERIMENTAL PROCEDURES

### Environmental sampling and isolation of strains

Water samples were collected during 2018–2020 in the Baltic Sea Proper. Samples were collected weekly at the K-station (56°39'25.4" N, 16°21'36.6" E, 1 m sampling depth), a coastal station in the Kalmar Sound, by the city of Kalmar, and every second week at the Linnaeus Microbial Observatory (LMO, 56°55'51.24" N, 17°3'38.52" E, 2 m sampling depth) situated 10 km off the east coast of Öland, Sweden. Temperature and salinity were measured using a conductivity/temperature/depth sensor CTD<sup>®</sup> Castaway at the K-station and a CTD probe (Alec Electronics, Japan) at LMO. To remove large particles, samples were filtered through a 200 µm mesh. For collecting environmental DNA samples, 200–400 mL seawater was filtered through a 47 mm 0.2 µm Supor<sup>®</sup>-200 filter (Pall Corporation, USA) using vacuum filtration. The filters were placed in cryotubes and stored at –80°C until extraction. Dissolved inorganic nutrients ( $\text{NO}_2^- + \text{NO}_3^-$ ,  $\text{PO}_4^{3-}$  and  $\text{SiO}_4^{4-}$ ) were measured as described in the study by

Alegria Zufia et al. (2022). Water aliquots for strain isolation were pre-filtered through a 3.0 µm polycarbonate filter, amended with  $\text{NO}_3^-$  (580 µM) and  $\text{PO}_4^{3-}$  (56.6 µM), and incubated for 24 h at 18, 16, or 20°C and  $15 \mu\text{mol m}^{-2} \text{s}^{-1}$  with a light: dark cycle of 12:12 h. After the incubation, picocyanobacteria were isolated by serial dilution in 24-well plates using L1 media (Guillard and Hargraves, 1993) prepared with Baltic Sea water with salinity ~7 PSU. Once the colour was visible in the well, cells were transferred to 40 mL plastic culture flasks and grown in L1 media prepared with artificial seawater (7 PSU), complemented with cycloheximide (final concentration of  $20 \text{ mg L}^{-1}$ ) to prevent eukaryote growth. The isolated strains are deposited, viable, and maintained in the Kalmar Algal Collection (KAC) at Linnaeus University, Sweden, and they are available upon request.

### Morphology and flow cytometry identification

The purity, defined as only one visual autotrophic morphotype, cell size, and morphology of the strains was examined using an epifluorescence microscope (Olympus BX50, country) equipped with filters for phycoerythrin (PE; 49010 ET Olympus BX2; 546 nm excitation 585 nm emission) and phycocyanin (PC; 49015 ET Olympus BX2; 605 nm excitation and 670 nm emission) at  $\times 1000$  magnification. The pigment content was examined using a CyFlow<sup>®</sup> Cube 8 flow cytometer (Partec<sup>®</sup>, Jettingen-Scheppach, Germany) as described in the study by Alegria Zufia et al. (2021). Briefly, forward scatter (FSC) was used as a proxy for cell diameter, FL2 (590/50 nm, blue laser dependent) as a proxy for PE content, FL3 (675/50 nm, blue laser dependent) as a proxy for Chl *a*, and FL4 (675/50 nm, red laser dependent) as a proxy for PC content.

### Molecular identification of strains

Samples for DNA were collected by harvesting 4 mL of each culture and centrifuging for 8 min at  $8000 \times g$  to form a cell pellet which was stored at –80°C until extraction. DNA was extracted using the FastDNA<sup>™</sup> SPIN Kit for Soil (MP Biomedicals) with Matrix E columns following manufacturer instructions with the addition of incubation with proteinase-K (1% final concentration) at 55°C for 1 h directly after the homogenization. DNA concentration was measured using an Invitrogen Qubit 2.0 fluorometer (Thermo Fisher Scientific Inc.) and purity was assessed using a Thermo Scientific<sup>™</sup> NanoDrop 2000 spectrophotometer (Thermo Fisher Scientific Inc.).

Strains were phylogenetically identified by amplifying and sequencing a fragment of the 16S rRNA gene

using universal primers 27F and 1492R (Lane, 1991). Given that *Synechococcus* is polyphyletic (Honda et al., 1999) and because sequences with equal percentage identities and query coverage can often be assigned to several genera (e.g. *Synechococcus* sp. and *Cyanobium* sp.), 16S rRNA gene sequences were used to assign taxonomy at the family level and to explore the phylogenetic placement of isolated strains within cluster 5 picocyanobacteria. The PC operon (subunit gene *cpcB*), and subunit genes *cpeBA* and *mpeBA* encoding PE-I and PE-II, respectively (Table S1) were used to assign pigment types. To design primers targeting *cpcB* and *mpeBA* genes, sequences of the beta (*cpcB*, *mpeB*) and alpha (*mpeA*) chains were obtained from whole genomes of *Synechococcus* strains available in the Cyanorak v2.1 database (<http://www.sb-roscoff.fr/cyanorak>). Sequences were aligned in MEGAX v.10.1.7 using the ClustalW algorithm (Stecher et al., 2020) and highly conserved regions were selected for primer design. The amplification reactions were carried out in 25 µL final volume reactions containing 10 ng of template DNA, 0.5 µM of each primer, and commercial PCR mix (Phusion High-Fidelity PCR Master Mix, Thermo Scientific) on a T100™ Thermal Cycler (Bio-Rad Laboratories, USA). The cycling conditions were initial denaturation at 98°C for 5 min, followed by 30 cycles at 98°C for 40 s, annealing temperature specific for each assay for 40 s, extension at 72°C for 1 min; and a final extension step at 72°C for 10 min (Table S1). PCR products were sequenced using Sanger sequencing (Macrogen Europe, Amsterdam, The Netherlands).

The 16S rRNA and pigment gene sequences were aligned with corresponding sequences obtained from cluster 5 picocyanobacterial genomes (Table S2) or selected phylogenetic studies (Schallenberg et al., 2022). Selected picocyanobacterial genomes were annotated using Prokka v. 1.14.6 (Seemann, 2014) using default settings plus ‘--compliant --rfam’, and all small subunit RNA sequences were extracted. For the pigment genes, amplicons obtained with the primers targeting *cpcB* and *cpeBA* genes were used as query sequences for BLASTn searches in the selected genomes using default parameters (Altschul et al., 1997). From the list of obtained hits, the ones with the best score in each genome were kept. Selected sequences were aligned with MAFFT v. 7.5 using the G-INS-I algorithm (with default parameters) (Kato et al., 2019) and used to generate maximum-likelihood phylogenetic trees using 1000 bootstraps in IQ-TREE v. 1.6.12 with default parameters (Hoang et al., 2018; Minh et al., 2020). ModelFinder was used to determine the best-fit model for each gene (Kalyaanamoorthy et al., 2017): GTR + F + I + I + R3 for the 16S rRNA, TIM3 + F + I + G4 for the *cpcB*, and TIM2e + I + G4 for the *cpeBA* gene sequences. Sequences generated in this study are

available in GenBank under the accession numbers OP441767-OP441783 for the 16S rRNA gene, OP484896 to OP484910 for *cpeB*, and OP484911 to OP484921 for *mpeBA* sequences.

## ASV libraries from environmental samples

Amplicon libraries were generated using the primers Cya-771F and Cya-1294R targeting the V5–V7 hyper-variable region (Huber et al., 2019) as described in the study by Alegria Zufia et al. (2022) and sequenced at SciLife using paired-end MiSeq 2 × 300 bp. The resulting reads were demultiplexed, denoised, and screened for chimera using amplicon (v1.1) which runs on QIIME2 (2019.10) and DADA2 (1.10.0). For relative abundances, only sequences affiliating with Synechococcales were included and are referred to as SYN below (see Alegria Zufia et al., 2022 for details). BLASTN searches were used to identify the ASVs with 100% nucleotide identity to the corresponding 16S rRNA gene fragment from the strains in this study. The sequence data is available in the NCBI Sequence Read Archive, BioProject PRJNA810944.

## Growth and pigment characterization of key strains under different temperature, light, and salinity conditions

Five strains (KAC 102, KAC 105, KAC 106, KAC 108, KAC 114), representing different phylogenetic clusters and pigment types (Figures 1 and 2) were chosen for further physiological characterization under a different light (10, 100, 190 µmol photons m<sup>-2</sup> s<sup>-1</sup> in 16:8 h, light:dark cycles), temperature (10, 15, 20, 25, 30°C) and salinity (2, 6, 10, 14 PSU) conditions. The light intensity of photosynthetic active radiation (PAR) was measured using an LI-COR spherical quantum meter (LI-189; LI-COR Inc., USA).

The in vivo pigment absorption spectra (400–750 nm) of the strains growing under 25°C, 10 µmol m<sup>-2</sup> s<sup>-1</sup>, and 6 PSU salinity were analysed with an Olis-modernized Cary 14 UV/Vis/NIR with Integrating Sphere upgrade spectrophotometer (On-Line Instrument Systems, Inc., Bogart, GA, USA) according to the method described by Blake and Griff (2012) with modifications. Briefly, first, a baseline with culture media was measured, and then 1 mL was replaced with cell suspension and measured.

Prior to the experiments, the strains were kept for 2 days in the experimental conditions for acclimatization (Śliwińska-Wilczewska et al., 2018). To start the experiments, cultures at the exponential phase were adjusted to a similar cell density (10<sup>5</sup> cells mL<sup>-1</sup>), and grown for 7 days in triplicates. Cell concentration was estimated from optical density (OD<sub>750 nm</sub>) using a



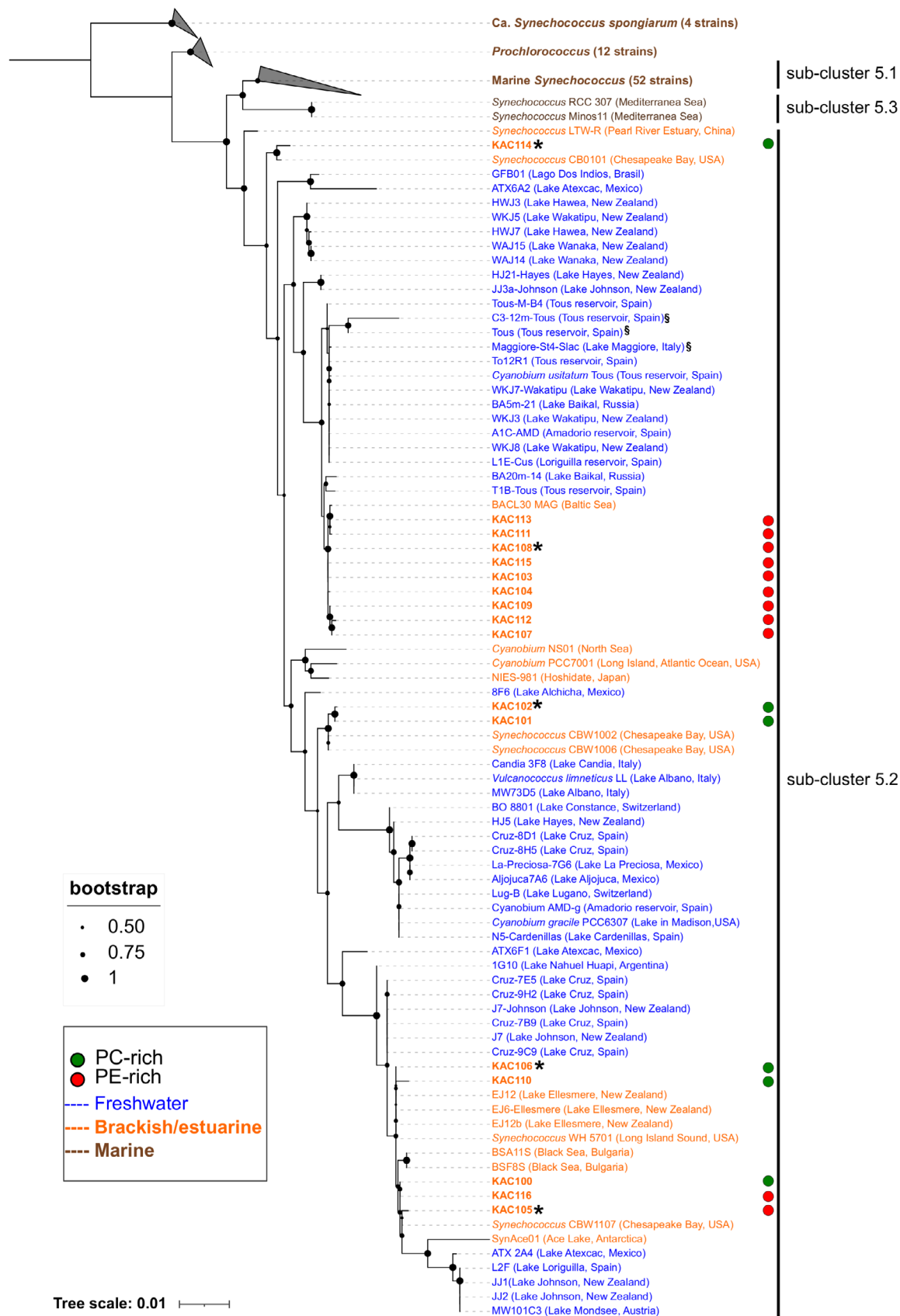


**FIGURE 1** Phylogenetic tree derived from partial 16S rRNA gene sequences using topology given by Maximum Likelihood (1000 bootstraps). Support values are indicated by the size of internal nodes. Strains isolated in this study are indicated in bold. Strains selected for further characterization are indicated with \*. The pigment phenotype is indicated by colours red (PE-rich) and green (PC-rich). § designate strains assigned to sub-cluster 5.3 based on multigene phylogenies (Cabello-Yeves, Callieri, et al., 2022; Cabello-Yeves, Scanlan, et al., 2022; Sánchez-Baracaldo et al., 2019).

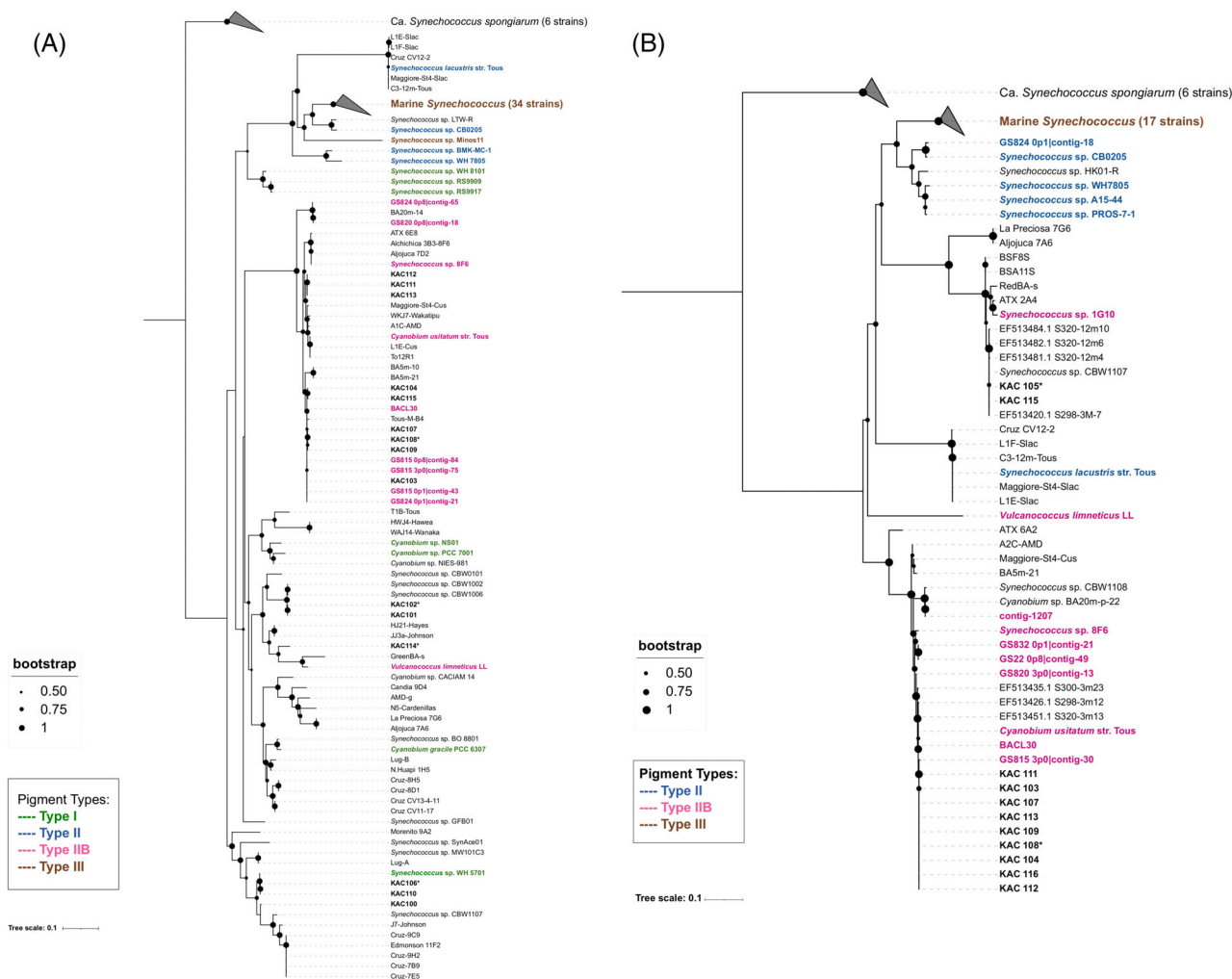


**FIGURE 2** Phylogenetic trees derived from *cpcB* (A) and *cpeBA* (B) gene sequences using topology given by maximum likelihood (1000 bootstraps). Support values for the branches are indicated by the size of internal nodes. Strains isolated in this study are indicated in bold. Strains selected for further characterization are indicated with\*. The trees include strains with characterized pigment types (Cabello-Yeves et al., 2018; Cabello-Yeves, Callieri, et al., 2022; Cabello-Yeves, Scanlan, et al., 2022; Grébert et al., 2018; Sánchez-Baracaldo et al., 2019; Six et al., 2007) and environmental sequences from the Baltic Sea (prefixed with GS, Larsson et al., 2014, EF Haverkamp et al., 2008, BACL 30, Hugerth et al., 2015).

Multiskan GO UV–VIS spectrophotometer (Thermo Scientific, Massachusetts, USA). OD<sub>750 nm</sub> showed a linear correlation with cell concentration determined by flow cytometry (BD Accuri C6 Plus; BD Biosciences, USA).

Chl *a* and carotenoids (Car) content was measured following Śliwińska-Wilczewska et al. (2018). Briefly, 5 mL of culture was filtered onto 0.45 µm filters (Macherey-Nagel MN GF-5, Macherey-Nagel GmbH & Co. KG, Düren, Germany), and Chl *a* and Car were extracted from cells with 90% acetone and incubated in the dark for 2 h at −20°C. The pigment extract was centrifuged at 17,700 × *g* for 2 min to remove filter particles (Sigma 2-16P, Osterode am Harz, Germany). Absorbance measurements were carried out in a 1 cm glass cuvette using a Multiskan GO UV–VIS spectrophotometer, at wavelengths (nm): 480, 665, and 750.

Chl *a* and Car concentration were calculated following Jeffrey and Humphrey (1975) and Strickland and Parsons (1968).

Phycobiliprotein content (PE, PC, and total Phycobilins) was measured following Śliwińska-Wilczewska et al. (2020). Briefly, 10 mL of culture was filtered through a 0.45 µm filter (Macherey-Nagel MN GF-5, Macherey-Nagel GmbH & Co. KG, Düren, Germany) and stored at −20°C. The reagent for phycobiliprotein extraction contained 0.25 M Trizma Base, 10 mM binary EDTA, and 2 mg mL<sup>−1</sup> lysozyme, pH of 5.5. Filters were homogenized in 5 mL of reagent and incubated first in the dark at 37°C for 2 h, then at 1.5°C for 20 h. Pigment extracts were centrifuged for 2 min, at 17,700 × *g* (Sigma 2-16P, Osterode am Harz, Germany). Absorption measurements were done on a Multiskan GO UV–VIS spectrophotometer, at

wavelengths (nm): 565, 620, 650, and 750. Phycobiliprotein content was calculated according to Bennett and Bogorad (1973) and Bryant et al. (1979).

Chl *a* fluorescence was measured with a pulse amplitude modulation (PAM) fluorometer (FMS1; Hansatech, King's Lynn, UK) following Śliwińska-Wilczewska et al. (2018). Samples were filtered through 13 mm diameter glass fibre filters (Whatman grade GF/C, GE Life Sciences, Mississauga, ON, Canada). Before measurement, filtered samples were kept in the dark for 5 min. The maximum quantum efficiency of photosystem II (PSII) was calculated as  $F_v/F_m$ , where  $F_v$  is the difference between maximum and minimum fluorescence and  $F_m$  is the maximum fluorescence (Campbell et al., 1998).

## Photosynthesis irradiance curves

Primary production was measured using the  $^{14}\text{C}$  method during the early exponential phase using a Photosynthetron (CHPT Manufacturing Inc.), with 24 incubation chambers, with PAR ranging from  $\sim 1$ – $2000 \mu\text{mol m}^{-2} \text{s}^{-1}$ . Prior to experiments, the strains were grown at 7 PSU in L1 media at 15 or  $20^\circ\text{C}$  at a light intensity of  $100 \mu\text{mol m}^{-2} \text{s}^{-1}$  with a light:dark cycle set to 12:12 for 7 days. The light gradient of each incubation chamber was measured with a quantum scalar irradiance meter (Biospherical Instruments Inc., QSL-100). For each chamber, glass vials with 0.5 mL of culture were amended with  $6 \mu\text{L } ^{14}\text{C}$ -bicarbonate ( $1 \mu\text{Ci}/\mu\text{L}$ ) and incubated. Two formalin-killed controls were included (3.3% final concentration). After 2 h, formalin was added to each of the remaining glass vials. Samples were filtered through 25 mm diameter  $0.22 \mu\text{m}$  black polycarbonate filters and the filters were incubated overnight in an acid fume chamber in the dark. A scintillation cocktail was added and the filters were incubated in the dark overnight and analysed using a liquid scintillation analyser (TriCarb 2100TR, Packard). The  $^{14}\text{C}$  incorporation was calculated using the equation:

$$\text{Photosynthesis } (\text{mgC m}^{-3} \text{h}^{-1}) = \frac{(\text{DPM}_{\text{sample}}) * 1.05 * \text{DIC}}{\text{DPM}_{\text{tot}} * t}$$

where  $\text{DPM}_{\text{sample}}$  is the amount of  $^{14}\text{C}$  in the sample,  $\text{DPM}_{\text{tot}}$  is the total amount of  $^{14}\text{C}$  that has been added to the sample.  $T$  is the incubation time (h), 1.05 is the preferred uptake of  $^{12}\text{C}$  over  $^{14}\text{C}$  and DIC is the amount of dissolved inorganic carbon (Johnson & Sheldon, 2007). DIC was calculated using the equation:

$$\text{mmol DIC/L} = ((0.43 + 0.156 * \text{salinity}) * 0.99) * F$$

where the salinity is the salinity of the culture media and  $F$  is a factor determined by pH, temperature, and

salinity conditions (Gargas, 1975). Photosynthesis–irradiance (P-I) curves for strain and temperature and the corresponding photosynthetic parameters were obtained after fitting the experimental data to the exponential model of Platt et al. (1980). Curve fitting was done in SPSS statistics v27.

## Statistical analyses

The relationship between the relative contribution of each of the identified ASVs to the total SYN community and environmental factors including dissolved inorganic nutrients, salinity, and temperature was analysed using Spearman's rank correlation test ( $n = 101$  after omitting NAs). Correlations were considered significant when  $\rho > 0.25$  and  $p$  after Bonferroni correction was  $p < 0.05$ . Multiple linear regression models were built in R 4.2.1, using the function `lm` (R Core Team, 2022) to determine the influence of variables (light, temperature, and salinity) on the growth rates of selected isolates (KAC 102, KAC 105, KAC 106, KAC 108, KAC 114). Three-way ANOVAs were used to test the effect of light, temperature, and salinity on cell abundance and pigment content using Statistica® 13.1. Data are presented as the mean  $\pm$  standard deviation of three replicates.

## RESULTS

### Characteristics of isolated strains

The colour of the 17 picocyanobacterial strains varied from blue-green to red-pink and brownish, indicating diversity in terms of pigment composition (Table 1). Flow cytometer analysis classified the strains according to their main pigment; PC-rich (six) and PE-rich strains (11). Under the microscope, several strains were observed to aggregate in microcolonies with a variable number of cells, from four to more than 10. Cell morphology ranged from nearly spherical to rod shape, and cell dimensions varied between strains ( $0.88$ – $2.20 \mu\text{m}$  cell diameter, Table 1).

### Molecular identification of strains

The phylogeny based on the *16S rRNA* gene (amplicon average 1385 bp) placed the new Baltic strains within the cluster 5 picocyanobacterial lineage, in sub-cluster 5.2 together with freshwater, estuarine and halotolerant strains, and separated from marine strains assigned to sub-clusters 5.1 and 5.3 (Figure 1). Based on this genetic marker, the strains were assigned to order Synechococcales and family Synechocaceae. Sequences had high identity ( $\sim 100\%$ ) with those from strains taxonomically assigned to either *Synechococcus* spp. or *Cyanobium* spp. The Baltic strains fell into

**TABLE 1** Characterization of cluster 5 picocyanobacteria isolated from the Baltic Sea proper. Temperature and salinity correspond to in situ values at the time of strain isolation measured with a CTD probe.

Strain	Isolation date/station	Temperature (°C)	Salinity (PSU)	Culture colour	Major phycobilin	Cell shape	Cell length (µm)	Cells forming microcolonies	ASV group
<b>KAC 106<sup>a</sup></b>	4 June 2019/K-Station	14.20	6.99	Green	PC	Spherical	1.35 ± 0.22	Yes	1
KAC 110	2 May 2018/K-Station	6.10	6.80	Green	PC	Spherical	1.30 ± 0.25	No	1
<b>KAC 108<sup>a</sup></b>	2 May 2018/LMO	6.10	6.80	Red	PE	Rod	1.41 ± 0.25	Yes	2
KAC 107	2 May 2018/LMO	6.10	6.80	Red	PE	Rod	1.4 ± 0.26	Yes	2
KAC 109	2 May 2018/LMO	6.10	6.80	Red	PE	Rod	1.21 ± 0.26	Yes	2
KAC 103	14 May 2019/K-Station	10.22	6.95	Red	PE	Spherical	1.02 ± 0.18	Yes	2
KAC 104	21 May 2019/K-Station	10.98	6.88	Red	PE	Rod	1.51 ± 0.26	Yes	2
KAC 115	21 May 2019/K-Station	10.98	6.88	Pink-red	PE	Rod	1.26 ± 0.22	Yes	2
<b>KAC 105<sup>a</sup></b>	28 May 2019/K-Station	13.49	6.92	Brownish-red	PE	Spherical	1.35 ± 0.27	No	3
KAC 116	2 April 2019/K-Station	5.39	6.89	Brownish-red	PE	Spherical	1.42 ± 0.19	No	3
<b>KAC 102<sup>a</sup></b>	19 March 2019/K-Station	3.67	6.82	Green	PC	Spherical	1.32 ± 0.18	Yes	4
KAC 100	19 March 2019/LMO	3.67	6.82	Green	PC	Spherical	1.23 ± 0.17	No	4
<b>KAC 114<sup>a</sup></b>	4 June 2019/K-Station	14.20	6.99	Green	PC	Spherical	1.57 ± 0.32	No	-
KAC 111	16 April 2019/K-Station	5.83	6.74	Red	PE	Rod	1.41 ± 0.30	Yes	-
KAC 112	16 April 16, 2019/K-Station	5.83	6.74	Orange-pink	PE	Rod	1.29 ± 0.24	Yes	-
KAC 113	21 May 2019/K-Station	10.98	6.88	Red	PE	Rod	1.15 ± 0.19	No	-
KAC 101	19 March 2019/K-Station	3.67	6.82	Green	PC	Spherical	1.26 ± 0.17	Yes	-

Abbreviations: LMO, Linnaeus Microbial Observatory; PC, phycocyanin; PE, phycoerythrin.

<sup>a</sup>Indicates strains selected for further characterization.



four main clusters, two composed of estuarine strains with local or fairly restricted distribution, and two with freshwater and brackish widespread strains: (i) PC-rich KAC 114 formed a well-supported cluster (100% bootstrap) with strain CB 0101, a representative strain of estuarine *Synechococcus*, isolated from the Chesapeake Bay (USA) (Fucich et al., 2019); (ii) nine out of 11 PE-rich strains fell in a widely distributed cluster composed of freshwater strains with diverse origin (e.g. Spain, Russia, New Zealand) and the widespread *Cyanobium usitatum* Tous among them (Cabello-Yeves et al., 2018; Cabello-Yeves, Callieri, et al., 2022; Cabello-Yeves, Scanlan, et al., 2022). Within this branch, the Baltic strains formed a well-supported separate cluster (95% bootstrap) with BACL30, a Baltic Sea metagenome-assembled genome (MAG) assigned to *Synechococcus* (Hugerth et al., 2015); (iii) PC-rich KAC 101 and KAC 102 formed another well-supported estuarine cluster (99% bootstrap) with cold-adapted *Synechococcus* sp. CBW1006 and CBW1002, isolated from the Chesapeake Bay (Xu et al., 2015); (iv) PC-rich (KAC 100, KAC 106, KAC 110) and PE-rich (KAC 105, KAC 116) were placed in another widespread cluster containing freshwater and estuarine strains such as the cold-adapted *Synechococcus* sp. CBW1107 isolated from Chesapeake Bay (Xu et al., 2015); euryhaline *Synechococcus* sp. WH5701 isolated from Long Island (USA) (Dufresne et al., 2008); marine/brackish strains from the Black Sea (BSF8S, BSA11S; Di Cesare et al., 2020) and Lake Ellesmere (EJ12, EJ6; Schallenberg et al., 2022), and freshwater strains from Lake Nahuel Huapi, North Patagonia (1G10; Sánchez-Baracaldo et al., 2019) and Lake Cruz (e.g. Cruz-7E5, Cruz 79B; Cabello-Yeves, Callieri, et al., 2022; Cabello-Yeves, Scanlan, et al., 2022). As expected, sub-cluster 5.3 marine strains *Synechococcus* RCC 307 and *Synechococcus* Minos 11 formed a well-supported clade separately from 5.2. Interestingly, recent whole sequenced freshwater strains assigned to sub-cluster 5.3 based on concatenated proteins (*S. lacustris* C3-12m-Tous; *S. lacustris* Tous, and *S. lacustris* Maggiore St4 Slac) (Cabello-Yeves, Callieri, et al., 2022; Cabello-Yeves, Scanlan, et al., 2022; Sánchez-Baracaldo et al., 2019) fell within sub-cluster 5.2 in our 16S rRNA gene phylogeny. This exemplifies the low resolution of the 16S rRNA as a marker when comparing even distantly related microbes such as *S. lacustris* and any of the strains from sub-cluster 5.32 that show ANI values of ca. 70%.

Primers targeting gene *cpcB* genes yielded the expected results for both PC- and PE-rich strains (Figure 2A). No amplification of *cpeBA* genes was observed for PC-rich strains (Type I). PE-rich strains contained *cpeBA* genes encoding PE-I, but no results were obtained when using primers targeting *mpeBA* genes encoding PE-II. However, when used with Type

III reference strains (WH 8102, CC 9311, and WH 7803), primers targeting *mpeBA* genes amplified expected products (data not shown). The phylogeny based on the *cpcB* gene placed the new Baltic strains separately from marine Type III strains (Figure 2A). PC-rich strains KAC 101, KAC 102, and KAC 114 fell in a relatively low supported cluster (57% bootstrap support) together with pigment Type I reference strains such as *Cyanobium* sp. PCC 7001, *Cyanobium* sp. NS01 and *Cyanobium gracile* PCC 6307. Unexpectedly, this branch also contained type IIB strain *V. limneticus* LL. The rest of the PC-rich strains (KAC 106, KAC 110, and KAC 100) fell in a well-supported cluster (99% bootstrap support) together with pigment Type I reference strain *Synechococcus* sp. WH 5701. PE-rich strains (except for KAC 105 and KAC 116 which were excluded from the analysis because the sequence was shorter than 400 bp) formed a well-supported cluster (100% bootstrap support) with strains and environmental sequences assigned to pigment Type IIB such as *Synechococcus* 8F6 and *C. usitatum* Tous, BACL30 MAG, and sequences from the Baltic Sea (prefixed with GS in Figure 2A). Phylogeny based on *cpeBA* sequences also separated strains isolated in this study from marine ones assigned to pigment Type III (Figure 2B). Nine out of 11 PE-rich strains were placed in a well-supported sub-cluster (100% bootstrap support) with freshwater strains assigned to pigment Type IIB (*Synechococcus* sp. 8F6 and *C. usitatum* Tous), one metagenome (BACL30) and environmental sequences from the Baltic Sea assigned to the same pigment type. KAC 105 and KAC 115 fell in another well-supported cluster (100% bootstrap support) with pigment Type IIB *Synechococcus* 1G10 and environmental sequences from the Baltic Sea assigned to the PE operon of uncultured cyanobacteria (prefixed with EF in Figure 2B).

## Environmental conditions and dynamics of ASVs

The 3-year time series (2018–2020) at the two Baltic Sea stations exhibited seasonal dynamics in both abiotic and biotic factors, being more pronounced at the coastal station (K-station; Figure 3). At the K-station, the temperature ranged from 0°C in winter to a peak of 24.4°C in the summer of 2018, while at the offshore station (LMO) the temperature ranged from 2.4°C in winter to a peak of 21.9°C in 2018 (Figure 3A). The mean salinity at both stations was 7 PSU, increasing seasonally from 6.4 in spring to 7.5 PSU in autumn at K-station, and ranging from 6.4 to 8 PSU at LMO with less clear seasonality (Figure 3B). In the gene amplicon libraries, four ASVs had 100% identity with the V7–V9 region of the 16S rRNA gene sequences of the strains (Group 1–4; Table 1). The four ASVs displayed

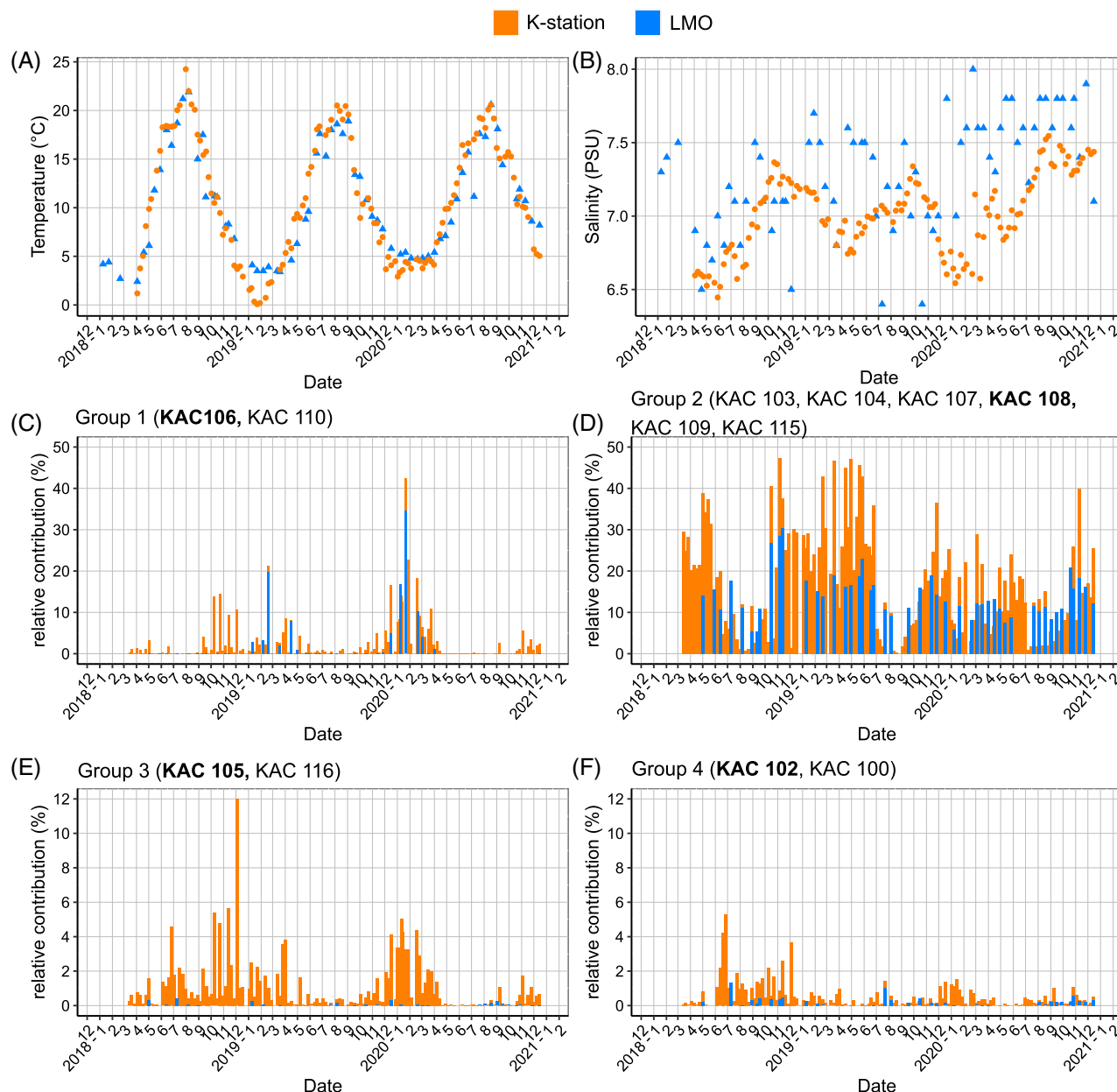


**FIGURE 3** Temperature (A), salinity (B), and relative abundance of ASVs at K-Station and LMO (C–F). The relative contribution of ASVs with 100% identity to the V5–V7 hypervariable region of the 16S rRNA gene sequence of the isolated strains.

different seasonality, contribution to the total picocyanobacterial community, and correlations with environmental factors (Figure 3C–F; Table S3). The four ASVs were found in libraries from both stations, but in general, their relative contribution was higher at the K-station. Group 1 (KAC 106 and KAC 110) increased by the end of autumn, peaked in winter (up to 20% and 40% relative SYN abundance in winter 2019 and 2020, respectively), decreased towards summer (Figure 3C). Accordingly, the contribution of Group 1 correlated negatively with temperature ( $\rho = -0.61$ ;  $p < 0.001$ ). The relative contribution of Group 2 (KAC 103, KAC 104, KAC 107, KAC

108, KAC 109, and KAC 115) was high throughout the sampling (up to 45% relative SYN abundance) but displayed lower relative contribution during the summer (3%–10% relative SYN abundance; Figure 3D). Compared to the others, this group was particularly important at LMO, where the contribution to the total picocyanobacterial population reached average 30% relative SYN abundance in autumn. The relative contribution of Group 2 correlated negatively with temperature ( $\rho = -0.42$ ;  $p < 0.001$ ). Group 3 (KAC 105 and KAC 116) was present mainly at the K-station. The average relative abundance was the highest during winter (~4% with a peak of 12% relative SYN

abundance in winter 2019; Figure 3E). The relative contribution of Group 3 correlated negatively with salinity ( $\rho = -0.36$ ;  $p < 0.001$ ). Group 4 (KAC 102 and KAC 100) had no clear seasonality and the relative abundance was  $<1\%$  at LMO and  $<2\%$  at K-station, except for the second half of the year 2019 when the contribution peaked at 4% relative SYN abundance (Figure 3F). The contribution of Group 4 correlated with neither temperature nor salinity but negatively with nitrate and positively with silicate (Table S3). An ASV identical to KAC 111, KAC 112, and KAC 113 was found at LMO and K-Station only during the second half of 2020 (data not shown). ASVs 100% identical to KAC 101 or 114 were not found in the environmental data from any of the stations.

### Growth and pigment characterization of selected strains under different conditions

Five strains were selected for further physiological characterization representing unique phylogenies and seasonality of ASVs (Figures 1 and 3, Table 1). In vivo light absorption peaked at  $\sim 565$  nm due to PE in the

red strains (KAC 105 and KAC108). In the green strains (KAC 102, KAC 106, and KAC 114), absorption spectra peaked at  $\sim 620$  nm due to PC. Chl *a* peaks were visible in the absorption spectra of both pigment phenotypes at 440 and 680 nm (Figure 4).

The five selected strains were able to grow in a wide range of temperature, light, and salinity conditions (Figure 5). The three factors had significant effects on cell numbers in the five strains (three-way ANOVA, Table S4) but influenced growth rates differently (Table 2, Table S5). Each strain exhibited a particular range of optimum conditions for best growth. None of the strains were able to grow at  $10^{\circ}\text{C}$ , the lowest tested temperature, during the 7-day incubations, but considering that some of the strains were isolated from samples with temperatures  $<10^{\circ}\text{C}$  (Table 1), it can be assumed that these picocyanobacteria can live at temperatures as low as that. For PC-rich KAC 102, the temperature was the strongest variable influencing growth (Table 2), and the strain displayed a temperature-dependent growth with an optimum of  $25^{\circ}\text{C}$  under the lowest light intensity ( $10 \mu\text{mol m}^{-2} \text{s}^{-1}$ ) and  $> 25^{\circ}\text{C}$  under higher light intensities. Growth rates were minimum under the lowest light intensity and

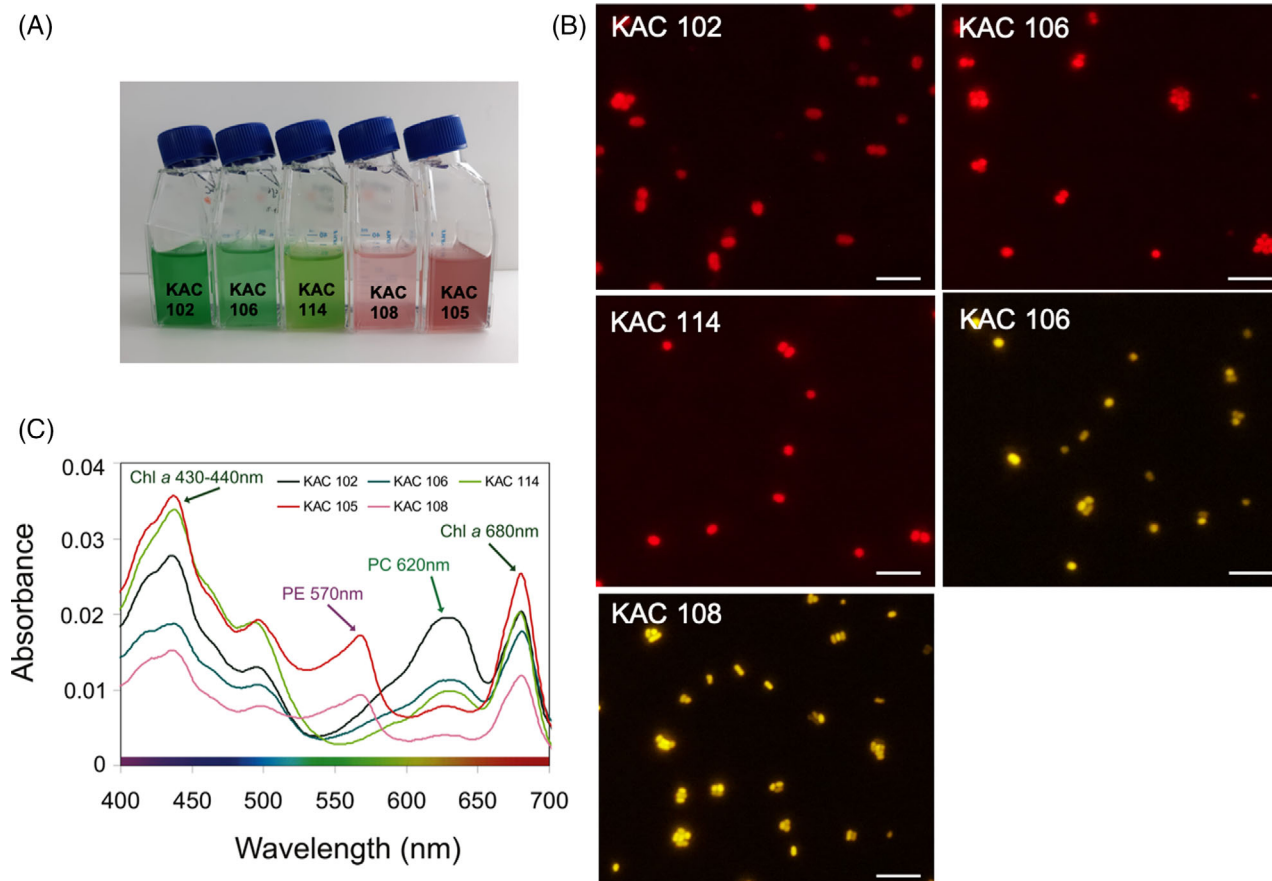


**FIGURE 4** Pigmentation and morphological diversity of selected strains isolated from the Baltic Sea Proper. (A) Pigmentation; (B) epifluorescence microscope micrograph; (C) pigment absorption spectra for PC-rich strains KAC 102 KAC 106, and KAC 114; PE-rich strains KAC 105 and KAC 108.

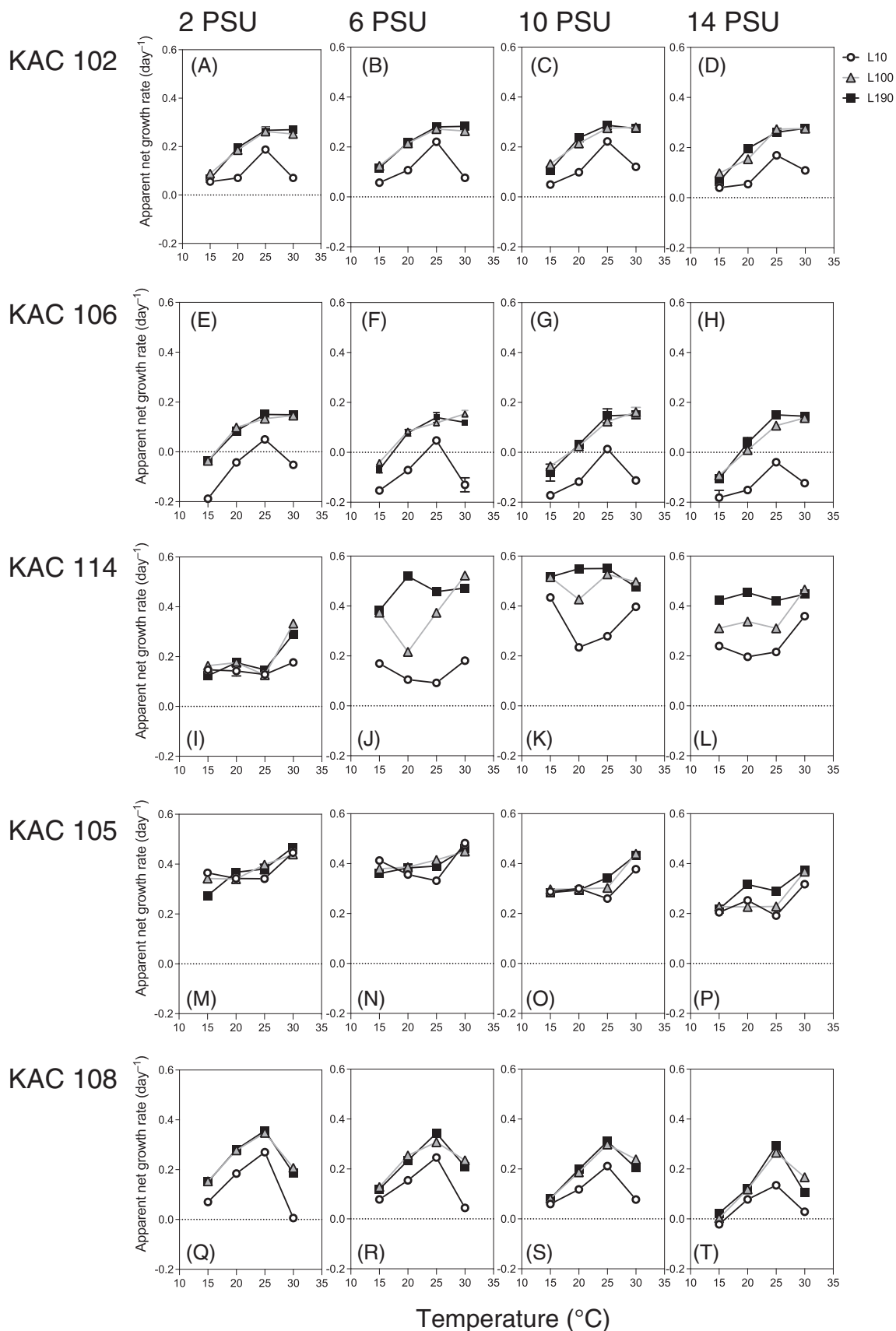


**FIGURE 5** Apparent net growth rates for selected strains isolated from the Baltic Sea Proper after 7 days of growth under different light, temperature, and salinity conditions. (A–D), KAC 102; (E–H), KAC 106; (I–L), KAC 114; (M–P), KAC 105; (Q–T), KAC 108. Error bars are standard deviations from the mean based on three replicates.



TABLE 2 Characteristics of selected picocyanobacterial strains and main factor influencing their growth under gradients of temperature, light and salinity.

Strain	Major phycobilin	Main factor influencing growth (adjusted $R^2$ and $p$ value for multiple linear regression models)	Pigment type (defined by <i>cpcB</i> , <i>cpeBA</i> phylogenies, and known pigment type representative strains)	Corresponding ASVs group, seasonality and correlation with environmental parameters	Closest strains physiologically characterized (based on the 16S rRNA gene phylogeny)
KAC 102	PC	Temperature > Light Adjusted $R^2 = 0.645$ , $p < 0.001$	I (Closest strain: <i>Cyanobium gracile</i> PCC 6307)	Group 4. No seasonality	<i>Synechococcus</i> CBW 1002, <i>Synechococcus</i> CBW 1006
KAC 106	PC	Temperature > Salinity > Light Adjusted $R^2 = 0.680$ , $p < 0.001$	I (Closest strain: <i>Synechococcus</i> sp. WH 5701)	Group 1 Autumn-winter. Negatively correlated with temperature	<i>Synechococcus</i> WH 5701
KAC 114	PC	Salinity > Temperature > Light Adjusted $R^2 = 0.525$ , $p < 0.001$	I (Closest strain: <i>Cyanobium gracile</i> PCC 6307)	Not found in environmental libraries	<i>Synechococcus</i> CB 0101
KAC 105	PE	Salinity > Temperature > Light Adjusted $R^2 = 0.651$ , $p < 0.001$	IIB (Closest strain: <i>Synechococcus</i> sp. 1G10)	Group 3. Dominant in winter. Negatively correlated with salinity	<i>Synechococcus</i> CBW 1107
KAC 108	PE	Temperature > Light > Salinity Adjusted $R^2 = 0.368$ , $p < 0.001$	IIB (Closest strain: <i>Synechococcus</i> sp. 8F6 and <i>Cyanobium usitatum</i> str. Tous)	Group 2. Dominant in autumn-spring. Negatively correlated with temperature	<i>Cyanobium usitatum</i> Tous

Abbreviations: PC, phycocyanin; PE, phycoerythrin.

similar under medium and high light intensity (100 and 190  $\mu\text{mol m}^{-2} \text{s}^{-1}$ , respectively) while similar apparent growth rates were registered under all salinities (Figure 5A–D). PC-rich KAC 106, displayed the same trends seen in KAC 102 in terms of temperature and salinity. The temperature was the strongest variable influencing its growth, followed by light (Table 2). The growth of KAC 106 was severely affected by low light (no growth) while the lowest limit for temperature tolerance was 15°C (Figure 5E–H). Growth in PC-rich KAC 114 was most influenced by light followed by salinity (Table 2). Apparent growth rates were similar under all tested temperatures but displayed a light-dependent growth, with the optimum under the highest light condition (Figure 5I–L). Maximum growth rates were observed under the highest salinities (PSU 6–14). This strain reached the highest growth rates among all the strains ( $0.55 \pm 0.01 \text{ day}^{-1}$  in PSU 10 and 25°C; Figure 5I–L). Salinity strongly influenced growth in PE-rich KAC 105 (Table 2). Apparent net growth rates increased slightly with temperature and were the highest at 30°C. This strain displayed a light-independent growth, but growth rates declined reciprocally with increasing salinity >10 PSU (Figure 5M–P). PE-rich KAC 108 displayed a temperature-dependent growth with an optimum at 25°C under all light and salinity conditions. Growth of KAC 108 was affected by low light (Table 2) as apparent net growth rates were the lowest for the lowest light intensity (10  $\mu\text{mol m}^{-2} \text{s}^{-1}$ ), but similar under 100 and 190  $\mu\text{mol m}^{-2} \text{s}^{-1}$ . Similar apparent growth rates were registered under all salinities (Figure 5Q–T).

Temperature, light, and salinity significantly influenced Chl *a* and Car content (three-way ANOVA, Tables S6 and S7). In general, the lowest Chl *a* content was registered under the highest light conditions, while Car content and Car to Chl *a* ratio increased with increasing light intensity (Figure 7, Figures S1 and S2). Chl *a* and Car content varied among strains, in some cases by one order of magnitude (Figures S2 and S3). Strain KAC 108, had the lowest Chl *a* and Car content (mean Chl *a*  $0.24 \pm 0.12 \text{ pg cell}^{-1}$ , mean Car  $0.30 \pm 0.11 \text{ pg cell}^{-1}$ ), while KAC 105 and KAC 106 accumulated the highest Chl *a* and Car content (up to  $3.00 \pm 1.23 \text{ pg Chl a cell}^{-1}$  and  $1.95 \pm 0.97 \text{ pg Car cell}^{-1}$  for KAC 106). Growth conditions led to different Car to Chl *a* ratios for different strains (Figure 6). In KAC 102, Car to Chl *a* ratios increased in high light but did not reach >1 and were relatively constant across temperatures and salinities (Figure 6A–D). In KAC 106, the highest light condition (190  $\mu\text{mol m}^{-2} \text{s}^{-1}$ ) led to Car to Chl *a* ratios >1 for all salinities and temperatures >20°C (Figure 6E–H). In KAC 114, the highest light condition led to ratios >1 for all salinities and temperatures (Figure 6I–L). PC-rich strains differed in their patterns of Car to Chl *a* ratios. In KAC 105, ratios >1 were observed only under high light intensities (100 and

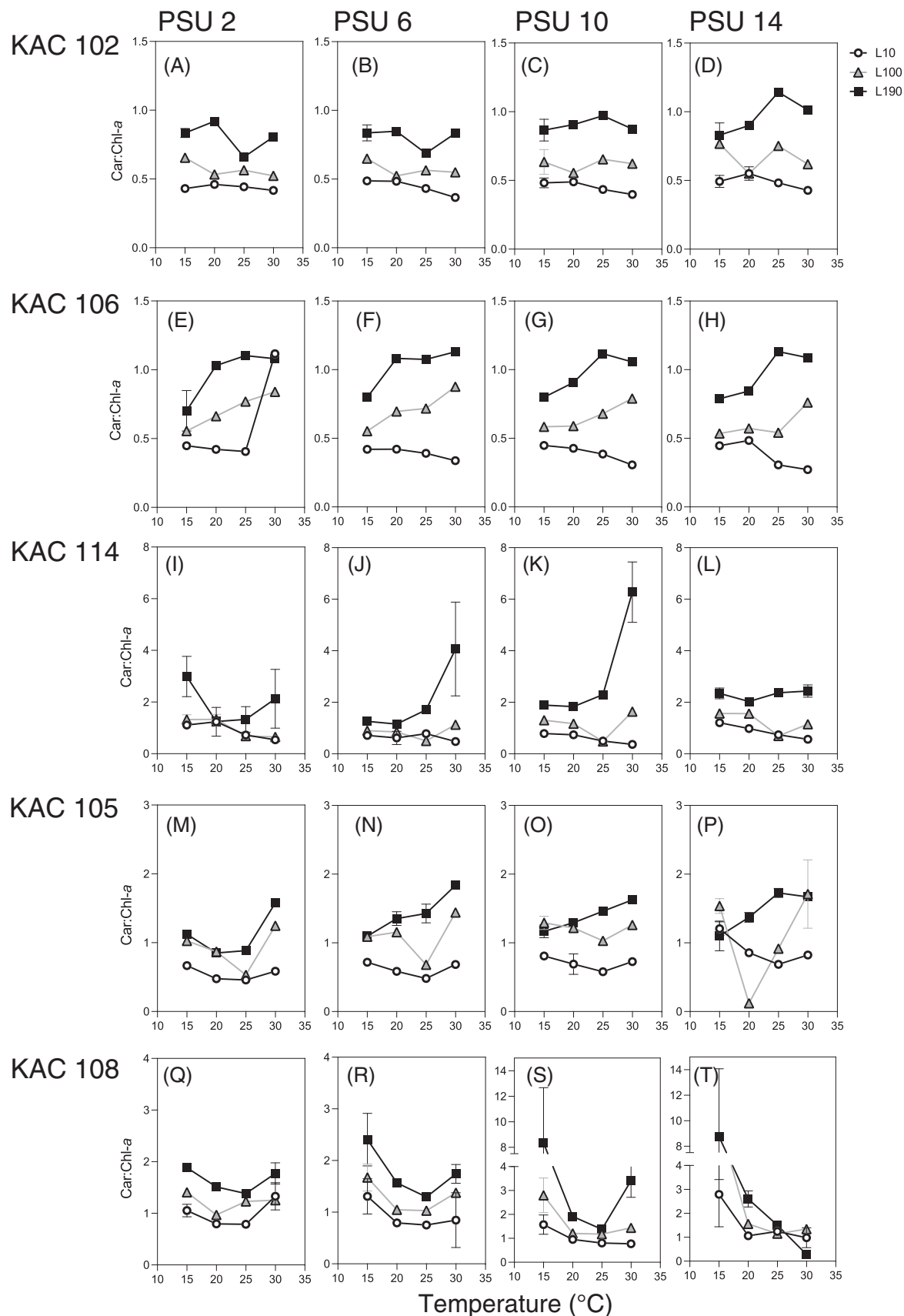


**FIGURE 6** Carotene: Chlorophyll-a content for the selected strains isolated from the Baltic Sea Proper after 7 days of growth under different light, temperature, and salinity conditions. (A–D), KAC 102; (E–H), KAC 106; (I–L), KAC 114; (M–P), KAC 105; (Q–T), KAC 108. Error bars are standard deviations from the mean based on three replicates.

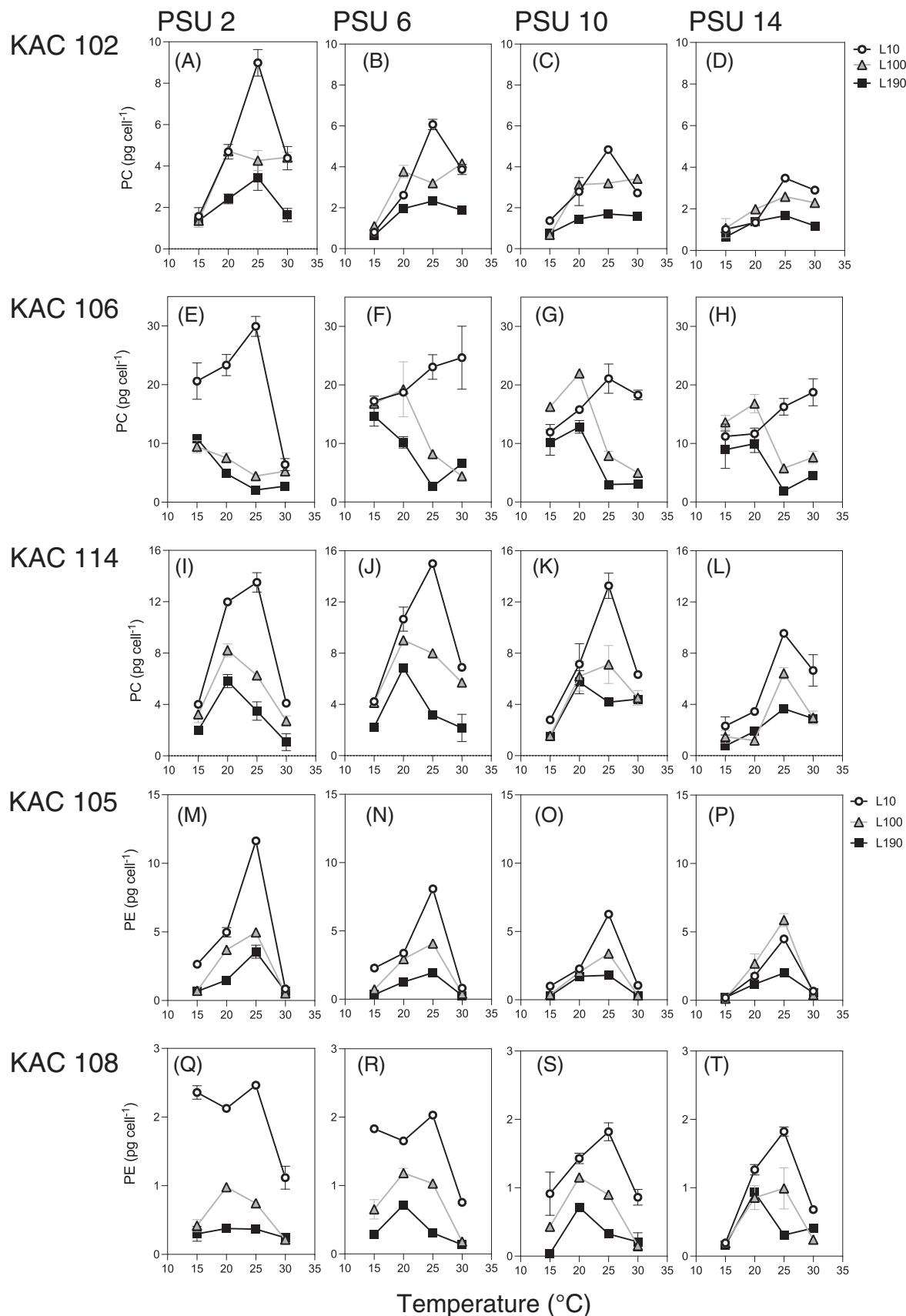


**FIGURE 7** Phycocyanin (A–P) and phycoerythrin (Q–T) content of selected strains isolated from the Baltic Sea Proper after 7 days of growth under different light, temperature, and salinity conditions. (A–D), KAC 102; (E–H), KAC 106; (I–L), KAC 114; (M–P), KAC 105; (Q–T), KAC 108. Error bars are standard deviations from the mean based on three replicates.

TABLE 3 Photosynthetic parameters obtained from the P-I curves.

Strain	Temperature of growth (°C)	$\alpha$	$\beta$	$P_{\max}$	$E_k$ ( $\mu\text{mol photon m}^{-2} \text{s}^{-1}$ )	Adjusted $R^2$ for exponential model
KAC 102	15	1.26E-10	3.04E-12	1.72E-08	136.1	0.841
KAC 102	20	2.14E-09	6.65E-11	3.72E-07	174.2	0.594
KAC 106	15	5.28E-11	2.75E-12	9.04E-09	171.2	0.53
KAC 106	20	2.16E-10	3.28E-12	2.88E-08	133.3	0.9
KAC 114	15	5.91E-12	4.17E-13	9.54E-10	161.2	0.72
KAC 114	20	1.39E-11	6.16E-13	1.46E-09	104.9	0.783
KAC 108	15	5.35E-11	1.31E-12	5.46E-09	102.0	0.774
KAC 108	20	5.71E-11	1.13E-12	9.10E-09	159.2	0.853

190  $\mu\text{mol m}^{-2} \text{s}^{-1}$ ) (Figure 6M–P). Almost all treatments led to Car to Chl *a* ratios >1 in KAC 108, even in the lowest light intensity (10  $\mu\text{mol m}^{-2} \text{s}^{-1}$ ) (Figure 6Q–T).

Temperature, light, and salinity significantly influenced PC and PE contents, which varied between strains (Tables S8 and S9). In general, the highest contents were observed under the lowest light intensity (10  $\mu\text{mol m}^{-2} \text{s}^{-1}$ ) and increased reciprocally with increasing temperature, peaking at 20 or 25°C (Figure 7). Among PC-rich strains, KAC 102 had the lowest average PC contents (min–max 0.57–9.40 pg. cell<sup>-1</sup>, mean 2.60 ± 1.64 pg. cell<sup>-1</sup>). In this strain, PC contents peaked under low-light intensity (10  $\mu\text{mol m}^{-2} \text{s}^{-1}$ ) and at 25°C in all salinities, while under higher light intensities, contents slightly increased with temperature (Figure 7A–D). KAC 106 had the highest PC contents (min–max 1.71–31.57 pg. cell<sup>-1</sup>, mean 11, 84 ± 7.15 pg. cell<sup>-1</sup>) showing peaks >20 pg. cell<sup>-1</sup> under low light and low salinity (2 and 6 PSU), while contents decreased with temperature increase under high light intensity (Figure 7E–H). KAC 114 accumulated intermediate contents (min–max 0.31–15.35 pg. cell<sup>-1</sup>, mean 5.26 ± 3.47 pg. cell<sup>-1</sup>) which peaked at 25°C under low light and at 20°C under 100 and 190  $\mu\text{mol m}^{-2} \text{s}^{-1}$  (Figure 7I–L). Among PE-rich strains, KAC 105 had the highest PE contents (min–max 0.07–11.71, mean 2.16 ± 2.31 pg. cell<sup>-1</sup>) which peaked at 25°C under all tested salinity and light conditions (Figure 7M–P). The average PE content in KAC 108 was one order of magnitude lower (min–max 0.03–2.52; mean 0.82 ± 0.64 pg. cell<sup>-1</sup>) and peaked at 25°C under low light and at 20°C under 100 and 190  $\mu\text{mol m}^{-2} \text{s}^{-1}$  (Figure 7Q–T).

P-I curves were analysed for PC-rich strains KAC 102, KAC 106, and KAC 114, and PE-rich KAC 108 growing in salinity 7 PSU at 15 and 20°C. P-I curves showed a marked difference in the photosynthetic characteristics of the strains under different temperatures (Figure S4). The highest maximum photosynthetic rates ( $P_{\max}$ ) and initial slopes ( $\alpha$ ) were observed at 20°C. Strains reached light saturation ( $E_k$ )

at different intensities and  $E_k$  showed no relation with temperature. KAC 102 and KAC 108 showed higher  $E_k$  when grown at 20°C and KAC 106 and KAC 114 when grown at 15°C (Table 3). Photoinhibition, determined by the parameter  $\beta$ , was strong for KAC 114 and observed >1000  $\mu\text{mol m}^{-2} \text{s}^{-1}$ . The other strains were much less sensitive to photoinhibition as they had lower  $\beta$  lower values, but photoinhibition was observed >1500  $\mu\text{mol m}^{-2} \text{s}^{-1}$  (Table 3, Figure S3).

Changes in the maximum quantum yield of photochemistry in PSII (determined as  $F_v/F_m$ ) provided further information on photoinhibition and acclimation. Treatments lead to significant changes in  $F_v/F_m$  (Table S10) but responses varied between strains (Figure S4). KAC 102 showed the greatest resistance to photoinhibition as it had the most constant  $F_v/F_m$  values regardless of growth conditions (Figure S4A–D). KAC 106, KAC 114, and KAC 115 were the most sensitive to photoinhibition as  $F_v/F_m$  declined reciprocally with increasing light intensity and temperature > 20°C. The highest temperature (30°) and light conditions (190  $\mu\text{mol m}^{-2} \text{s}^{-1}$ ) led to the greatest reductions in  $F_v/F_m$ . These patterns were relatively consistent across salinities (Figure S4E–P). KAC 108 exhibited relatively constant  $F_v/F_m$  values under all conditions (no trend identified; Figure S4Q–T).

## DISCUSSION

The present work combining molecular characterization and field observations with physiological studies using a wide range of conditions revealed the occurrence of genetically distinct picocyanobacterial populations exhibiting different environmental preferences. The eco-physiological studies evidenced distinct responses in closely related strains, showing that phylogenetic grouping based on 16S rRNA gene sequences conceals considerable physiological diversity. Moreover, the tracking of amplicon sequencing data over 3 years showed temporal differences in population dynamics, supporting that the strains studied here represent key



ecotypes among the diverse Baltic Sea picocyanobacterial populations. These ecotypes would occupy distinct ecological niches likely defined by temperature, light, and salinity (discussed below). In addition, the present study highlights a previously overlooked functional diversity among estuarine PE- and PC-rich picocyanobacterial populations, suggesting that understanding the ecology of estuarine picocyanobacteria requires analysis beyond the phycocyanin and phycoerythrin divide. Altogether, these results expand our knowledge of the diverse yet understudied sub-cluster 5.2 (Cabello-Yeves, Callieri, et al., 2022; Cabello-Yeves, Scanlan, et al., 2022; Callieri et al., 2013, 2022) and substantially refine our knowledge of the dynamics and diversity of co-occurring picocyanobacterial lineages in estuarine systems. The rearrangement of accessory genes provides cluster 5 picocyanobacteria with a selective advantage to adapt to changing environments, contributing to its plasticity and adaptability to different aquatic ecosystems (Callieri, 2017). In particular, larger genomes with a larger set of flexible genes would enable freshwater cluster 5 picocyanobacteria to adapt and thrive in a wide number of ecological niches (Cabello-Yeves, Callieri, et al., 2022; Cabello-Yeves, Scanlan, et al., 2022). In the future, genome sequencing of these new Baltic strains will allow further characterization of estuarine genomes (gene presence/absence, gene synteny, and genomic island prediction) enabling the exploration of niche colonization and links between the ecology and evolution of estuarine picocyanobacteria.

Contrary to the marine counterparts, the phylogeny of estuarine and freshwater cluster 5 picocyanobacteria remains unclear. In the present study, the combined use of four molecular marker genes (16S rRNA, *cpcB*, *cpeBA*, and *mpeBA*) provided complementary insights into the diversity and ecophysiology of estuarine picocyanobacteria. The position of the Baltic strains in the 16S rRNA gene phylogeny confirmed the placement of estuarine strains outside marine sub-cluster 5.1. It also reinforces the placement of estuarine and freshwater strains in sub-cluster 5.2, in line with recent 16S rRNA gene phylogenies (Schallenberg et al., 2022) and phylogenomic trees using concatenated proteins (Cabello-Yeves, Callieri, et al., 2022; Cabello-Yeves, Scanlan, et al., 2022; Sánchez-Baracaldo et al., 2019) from cultured cluster 5 picocyanobacteria. The position of the strains isolated in this study in four different clusters points to the coexistence of (i) local populations adapted to estuarine conditions and (ii) populations in the transition from the marine/brackish environment to a freshwater environment, with a broader distribution. For instance, the well-supported clade containing the Baltic PC-rich strains together with freshwater *Synechococcus* and *Cyanobium* strains, and *Cyanobium* sp. BACL30 MAG (Hugerth et al., 2015) points to evolutionary links between freshwater lineages and the Baltic

brackish microbiome (Alegria Zufia et al., 2022; Sánchez-Baracaldo et al., 2008). *Cyanobium* BACL30 MAG is closely related to *Cyanobium usitatum* Tous (93% ANI), a widely distributed freshwater picocyanobacterium and abundant in cold waterbodies and temperate reservoirs (Cabello-Yeves et al., 2018). On the other hand, the position of strains in strictly estuarine clusters (e.g. KAC 114, KAC 102, and KAC 101) together with representative estuarine strains isolated from the Chesapeake Bay (e.g. CB0101, CBW1002, CBW 1006) suggest local adaptations. It may also indicate that the Baltic strains count with the ecophysiological features seen in the above-mentioned representative estuarine strains to thrive in highly dynamic environments (Fucich et al., 2019, 2021). It is noteworthy that some of the 16S rRNA gene sequences obtained from the strains were not found in 3-year amplicon libraries. Likewise, the set of strains isolated in this study did not fully cover the diversity revealed by the picocyanobacterial ASVs. This points out that complementary approaches are needed to assess the diversity of picocyanobacteria. Finally, it is worthy to underline that a more detailed genetic study involving not only the 16S rRNA gene, but the whole genome could potentially give a different picture of the phylogenetic relationship of cluster 5 picocyanobacteria.

Previous analysis based on 16S rRNA gene sequences recognize several clusters within or closely related to sub-cluster 5.2, such as Subalpine cluster II, Bornholm Sea cluster, clade B (Crosbie et al., 2003; Ernst et al., 2003; Huber et al., 2019; Xu et al., 2015). Each cluster exhibits specific morphological features. For instance, variable cell length was registered in *Synechococcus* strains falling within the Bornholm Sea cluster (Ernst et al., 2003; Xu et al., 2015) while strains assigned to Subalpine cluster II had nearly spherical to short rod shapes (Xu et al., 2015). While the Baltic Sea strains fell in different branches in our 16S rRNA gene phylogeny, we found no consistent pattern between phylogeny and cell morphology (i.e., cells with both rod and spherical shapes were found in all lineages). This could be due to that our studied strains encompassed a broad variety of morphologies (and physiologies; see below), although some degree of plasticity in morphology could also play a part. It should also be noted that morphology and morphotypes are not stable forms. For example, single cells can aggregate (or remain attached) and form microcolonies under the presence of heterotrophic bacteria, grazing pressure, or exposure to UV radiation (Callieri et al., 2011; Cruz & Neuer, 2019; Ospina-Serna et al., 2020).

The analysis of pigment genes (*cpcB*, *cpeBA*, and *mpeBA*) evidenced an assembly of pigment diversity in the Baltic Sea Proper (Type I and Type IIB; Six et al., 2007; Larsson et al., 2014) which is ecologically relevant as strains with different pigmentation can grow

under different underwater light conditions (Callieri, 2017; Haverkamp et al., 2008, 2009; Stomp et al., 2007; Xia et al., 2017). Phylogenies based on pigment genes also supported the separation of the Baltic strains from the pelagic-marine strains and expanded our knowledge of pigment Type distribution. The absence of *mpeBA* genes encoding PE-II in the Baltic strains agrees with recent genomic studies of freshwater and brackish picocyanobacteria (Cabello-Yeves, Callieri, et al., 2022; Cabello-Yeves, Scanlan, et al., 2022). Together with the global analysis of pigment Type distribution (Grébert et al., 2018), our study indicates that pigment Type III strains are rarely found in estuarine systems. The identification of strains with pigment Type IIB, which dominates the brackish areas of the Baltic Sea throughout the summer (Larsson et al., 2014), allows for the assessment of the ecophysiology of this novel pigment Type (discussed below). While considered absent in open oceans strains, the presence of pigment Type IIB in freshwater picocyanobacterial strains (e.g. *C. usitatum* Tous; *Synechococcus* sp. 8F6, *Synechococcus* sp. 1G10; Cabello-Yeves et al., 2018; Sánchez-Baracaldo et al., 2019) suggests a link between freshwater and estuarine strains. Finally, the disposition of the PE-rich strains in two separate and well-supported clusters containing different Type IIB representative strains in each of them, suggests a previously unnoticed diversity within pigment Type IIB that requires further exploration.

Global ocean studies show an overall positive relationship between *Synechococcus* growth rates, abundance, and temperature (Flombaum et al., 2020; Hunter-Cevera et al., 2016; Visintini et al., 2021). Recent models of niche partitioning along temperature gradients predict increases in *Synechococcus* biomass with temperatures between 20°C and 30°C (Flombaum et al., 2020). In this study, temperature strongly affected the growth but strains displayed different temperature optima. KAC 108, KAC 102, and KAC 106 displayed the traditional temperature-dependent growth curve as seen in other picophytoplankton including *Synechococcus* and *Prochlorococcus* isolates (Kulk et al., 2012; Pittera et al., 2014; Six et al., 2021; Stawiarski et al., 2016). The optimum temperatures for these strains (25–30°C) were similar to those reported for marine *Synechococcus* isolated from high and mid-latitudes (Pittera et al., 2014), and PC-rich and PE-rich *Synechococcus* strains from the Baltic Sea (Śliwińska-Wilczewska et al., 2018). In contrast, no clear optimum temperature was observed for KAC 114, while growth rates slightly increased towards 30°C in KAC 105 indicating that the optimum temperature for these two strains was above 25–30°C, as reported for more tropical *Synechococcus* strains (Pittera et al., 2014; Six et al., 2021). Our results suggest a potential advantage for some of the strains to increase their biomass contribution as a consequence of their differences in

temperature optima and tolerance ranges. Thus, ongoing climate warming (HELCOM, 2021) will largely influence the abundance and composition of the cluster 5 picocyanobacterial community.

Light preference in *Synechococcus* strains is intimately linked to seasonality, distribution in the water column, biogeography, and phylogeny (Ahlgren & Røcap, 2006; Mackey et al., 2017). While light was an important factor determining growth, strains isolated in this study showed strong differences in light preferences and photoinhibition, which was associated with pigment content and photosynthetic performances. Observed responses, ranging from light intensity-dependent growth (PC-rich KAC 102 and KAC 106, and PE-rich KAC 108), strong photoinhibition under high light intensities (PE-rich KAC 114), to light intensity-independent growth (PE-rich KAC 105), suggest that distinct photo-physiological ecotypes co-occur in the Baltic Sea. Pigment Type composition could explain the distinct light preferences observed in PE-rich KAC 108 and KAC 105. Even though they were both assigned to pigment Type IIB, their position in the phylogenetic trees (i.e., e in two separate clusters) suggests further variability in this pigment Type, which could be reflected in different tolerances to low light, and supporting the coexistence of PE-rich populations with different light adaptations. Accordingly, recent studies revealed a continuum of light responses in marine *Synechococcus*, ranging from low-light optimized to high light-optimized strains, which was tightly linked to phylogeny and pigmentation (Mackey et al., 2017). Under climate change, more pronounced stratification due to rising temperatures, enhanced eutrophication, and brownification are expected to alter underwater light regimes (Wollschläger et al., 2021). In light of our results, responses to these effects can emerge as alterations in the physiology, composition, and biomass of co-occurring strains.

Pigment composition separates ecological niches along spectral gradients (Stomp et al., 2004, 2007) and may indicate the level of acclimatization of cyanobacteria to specific environmental conditions (Takaichi & Mochimaru, 2007). The degree of plasticity under different conditions impacts the distribution, coexistence, and succession in marine *Synechococcus* (Mackey et al., 2017; Pittera et al., 2014). In this study, strains with similar phycobilin composition (i.e., PC-rich or PE-rich) exhibited large differences in pigment content per cell (PE, PC, Chl *a*, and carotenoids). These differences could be attributed to variations in cell biovolumes among strains or differences in the thylakoid membrane surfaces. Notably, strains isolated under the lowest temperatures (KAC 108 and KAC 102) exhibited the lowest pigment content, while strains isolated under higher temperatures (e.g. KAC 106 and KAC 105) showed the opposite trend. This points to a link between pigment content and the temperature of the

isolation site, as seen in marine *Synechococcus* isolated from different latitudes (Pittera et al., 2014).

In this study, light-harvesting pigments content (PE, PC, and Chl *a*) generally decreased under higher light. This can be explained by cells requiring less photosynthetic apparatus under higher light conditions and also as a way to protect the photosynthetic machinery against oxygen radical formation (Richardson et al., 1983). Pigments with photoprotective functions such as carotenoids tend to increase under high light and can be used as a proxy for oxidative stress (Goerick & Montoya, 1998; Masamoto & Furukawa, 1997). Carotenoid content varied under tested conditions, from increases in parallel with increases in light (e.g. KAC 102, KAC 108) to similar contents across gradients (e.g. in KAC 106). The observed array of responses highlights that strains can acclimate to changing environments by changing pigment content, illustrating their high adaptability.

In the Baltic Sea, the picocyanobacterial composition is strongly correlated with salinity, and the distribution of populations, from brackish to marine ones, correlates with the presence of genes involved in salt acclimation (Celepli et al., 2017; Hu et al., 2016; Larsson et al., 2014). Strains isolated in this study exhibited contrasting responses to salinity gradients, ranging from wide salinity tolerance (PE-rich 108, PC-rich KAC 102, and KAC 106), to positive influence by low (PE-rich KAC 105) or high salinity (PE-rich KAC 114). This was congruent with the environmental preferences of the correspondent ASVs in the field. The ability to grow successfully over the tested gradient (2–14 PSU) is notable since salinity in the Baltic Sea Proper where strains were isolated, ranges from 6 to 8 PSU (Larsson et al., 2014). PE-rich 108 (wide salinity tolerance) showed high sequence identity to *C. usitatum* Tous (93% ANI), a freshwater specialized picocyanobacterium given its broad distribution in multiple cold and temperate waters, and optimal growth in salinities <3 PSU (Cabello-Yeves et al., 2018). Interestingly, genomic searches of *C. usitatum* Tous revealed the presence of several transporters (e.g. electrochemical potential-driven channels, transporters for polar amino acids and proline/betaine, glutamate:Na<sup>+</sup> and glucose/mannose:H<sup>+</sup> symporters) that could help to explain their presence in low salinity regions of the Baltic Sea (Cabello-Yeves et al., 2018). Recent genomic studies in *Synechococcus* evidenced that sets of compatible solute biosynthetic pathways are not homogeneously distributed among 18 brackish strains (Cabello-Yeves, Callieri, et al., 2022; Cabello-Yeves, Scanlan, et al., 2022), pointing to different tolerances and adaptability to salinity gradients. Future phylogenomic analyses interrogating the evolutionary trajectories of selected strains (e.g. whether phylogenetic clades correlate with osmolyte repertoires) will provide novel insights into salinity range adaptations of estuarine cluster 5 picocyanobacteria.

## CONCLUSIONS

Climate change is expected to modify abiotic and biotic drivers in aquatic environments. Consequences of climate change are already seen in the coastal waters of the Baltic Sea (HELCOM, 2021) and global predictions are that picocyanobacteria will increase in abundance at higher latitudes (Flombaum et al., 2020). However, our study highlights the interplay between temperature, irradiance, and salinity in leading differential pigment content, photosynthetic adjustments, and growth in picocyanobacterial strains, therefore favouring specific picocyanobacterial ecotypes.

In addition, the functional diversity found within strains with the same dominant pigment type underscores that other intrinsic characteristics apart from the pigment composition determine successful growth in estuarine PC-rich and PE-rich picocyanobacteria. In the future, genome sequencing of these novel strains will allow further exploration of links between the ecology and evolution of estuarine picocyanobacteria.

## AUTHOR CONTRIBUTIONS

**Anabella Aguilera:** Formal analysis (lead); investigation (lead); methodology (lead); visualization (lead); writing – original draft (lead); writing – review and editing (lead). **Javier Alegria Zufia:** Formal analysis (equal); methodology (equal); visualization (equal); writing – review and editing (equal). **Laura Bas Conn:** Methodology (equal). **Leandra Gurli:** Methodology (equal). **Sylwia Śliwińska-Wilczewska:** Formal analysis (equal); methodology (equal); visualization (equal). **Gracjana Budzałek:** Methodology (equal). **Daniel Lundin:** Formal analysis (supporting); methodology (equal). **Jarone Pinhassi:** Funding acquisition (equal); supervision (supporting); writing – review and editing (equal). **Catherine Legrand:** Funding acquisition (equal); supervision (supporting); writing – review and editing (equal). **Hanna Farnelid:** Conceptualization (lead); funding acquisition (lead); supervision (lead); writing – original draft (equal); writing – review and editing (equal).

## ACKNOWLEDGEMENTS

The authors would like to thank technical employees within EEMiS that have made sampling at K-station and LMO possible, Kalmar Kommun for access to Kallbadhuset and RWE Kårehamn Windpark, Northern Off-shore Services (NOS), and the Provider crew for technical assistance during sampling at LMO. We also thank Douglas A. Campbell for providing laboratory equipment. High-throughput amplicon sequencing was performed by the SNP&SEQ Technology Platform in Uppsala. The facility is part of the National Genomics Infrastructure (NGI) Sweden and Science for Life Laboratory. The SNP&SEQ Platform is also supported by the Swedish Research Council and the Knut and Alice Wallenberg Foundation.



## FUNDING INFORMATION

This work was supported by FORMAS (2017-00468) and Anna-Greta and Holger Crafoord Foundation (CR2019-0012) to Hanna Farnelid, the Knut and Alice Wallenberg Foundation (570630-3095 to Hanna Farnelid and Jarone Pinhassi), the Strategic Research Programme Ecochange (Research Council FORMAS to Catherine Legrand and Jarone Pinhassi), the Canada Foundation for Innovation and the New Brunswick Innovation Foundation.


## CONFLICT OF INTEREST STATEMENT

None declared.

## DATA AVAILABILITY STATEMENT

Sequences generated in this study are available in GenBank under the accession numbers OP4417 67-OP441783 for the 16S rRNA gene, OP484896 to OP484910 for *cpeB*, and OP484911 to OP484921 for *mpeBA* sequences. 16S rRNA sequences from environmental samples are available in the NCBI Sequence Read Archive, BioProject PRJNA810944.

## ORCID

Anabella Aguilera  <https://orcid.org/0000-0001-6743-3001>

Daniel Lundin  <https://orcid.org/0000-0002-8779-6464>

## REFERENCES

- Ahlgren, N. & Røcap, G. (2012) Diversity and distribution of marine *Synechococcus*: multiple gene phylogenies for consensus classification and development of qPCR assays for sensitive measurement of clades in the ocean. *Frontiers in Microbiology*, 3, 213.
- Ahlgren, N.A. & Røcap, G. (2006) Culture isolation and culture-independent clone libraries reveal new marine *Synechococcus* ecotypes with distinctive light and N physiologies. *Applied and Environmental Microbiology*, 72, 7193–7204.
- Alegria Zufia, J., Farnelid, H. & Legrand, C. (2021) Seasonality of coastal picophytoplankton growth, nutrient limitation, and biomass contribution. *Frontiers in Microbiology*, 12, 3674.
- Alegria Zufia, J., Legrand, C. & Farnelid, H. (2022) Seasonal dynamics in picocyanobacterial abundance and clade composition at coastal and offshore stations in the Baltic Sea. *Scientific Reports*, 12, 14330.
- Altschul, S.F., Madden, T.L., Schaffer, A.A., Zhang, J., Zhang, Z., Miller, W. et al. (1997) Gapped BLAST and PSI-BLAST: a new generation of protein database search programs. *Nucleic Acids Research*, 25, 3389–3402.
- Bennett, A. & Bogorad, L. (1973) Complementary chromatic adaptation in a filamentous blue-green alga. *The Journal of Cell Biology*, 58, 419–435.
- Bertos-Fortis, M., Farnelid, H.M., Lindh, M.V., Casini, M., Andersson, A., Pinhassi, J. et al. (2016) Unscrambling cyanobacteria community dynamics related to environmental factors. *Frontiers in Microbiology*, 7, 625.
- Blake, R.C. & Griff, M.N. (2012) In situ spectroscopy on intact leptospirillum ferrooxidans reveals that reduced cytochrome 579 is an obligatory intermediate in the aerobic iron respiratory chain. *Frontiers in Microbiology*, 3, 136.
- Bryant, D.A., Guglielmi, G., de Marsac, N.T., Castets, A.-M. & Cohen-Bazire, G. (1979) The structure of cyanobacterial phycobilisomes: a model. *Archives of Microbiology*, 123, 113–127.
- Cabello-Yeves, P.J., Callieri, C., Picazo, A., Schallenberg, L., Huber, P., Roda-Garcia, J.J. et al. (2022) Elucidating the picocyanobacteria salinity divide through ecogenomics of new freshwater isolates. *BMC Biology*, 20, 175.
- Cabello-Yeves, P.J., Haro-Moreno, J.M., Martin-Cuadrado, A.-B., Ghai, R., Picazo, A., Camacho, A. et al. (2017) Novel *Synechococcus* genomes reconstructed from freshwater reservoirs. *Frontiers in Microbiology*, 8, 1151.
- Cabello-Yeves, P.J., Picazo, A., Camacho, A., Callieri, C., Rosselli, R., Roda-Garcia, J.J. et al. (2018) Ecological and genomic features of two widespread freshwater picocyanobacteria. *Environmental Microbiology*, 20, 3757–3771.
- Cabello-Yeves, P.J., Scanlan, D.J., Callieri, C., Picazo, A., Schallenberg, L., Huber, P. et al. (2022)  $\alpha$ -Cyanobacteria possessing form IA RuBisCO globally dominate aquatic habitats. *The ISME Journal*, 16, 2421–2432.
- Callieri, C. (2017) *Synechococcus* plasticity under environmental changes. *FEMS Microbiology Letters*, 364, fnx229.
- Callieri, C., Cabello-Yeves, P.J. & Bertoni, F. (2022) The “dark side” of picocyanobacteria: life as we do not know it (yet). *Microorganisms*, 10, 546.
- Callieri, C., Coci, M., Corno, G., Macek, M., Modenutti, B., Balseiro, E. et al. (2013) Phylogenetic diversity of nonmarine picocyanobacteria. *FEMS Microbiology Ecology*, 85, 293–301.
- Callieri, C., Lami, A. & Bertoni, R. (2011) Microcolony formation by single-cell *Synechococcus* strains as a fast response to UV radiation. *Applied and Environmental Microbiology*, 77, 7533–7540.
- Callieri, C., Mandolini, E., Bertoni, R., Lauceri, R., Picazo, A., Camacho, A. et al. (2021) Atlas of picocyanobacteria monoclonal strains from the collection of CNR-IRSA Italy. *Journal of Limnology*, 80, 2002.
- Callieri, C. & Stockner, J.G. (2002) Freshwater autotrophic picoplankton: a review. *Journal of Limnology*, 61, 1–14.
- Campbell, D., Hurry, V., Clarke, A.K., Gustafsson, P. & Oquist, G. (1998) Chlorophyll fluorescence analysis of cyanobacterial photosynthesis and acclimation. *Microbiology and Molecular Biology Reviews*, 62, 667–683.
- Castenholz, R.W. (2001) Phylum BX. Cyanobacteria. In: En Boone, D.R., Castenholz, R.W. & Garrity, G.M. (Eds.) *Bergey's manual of systematic bacteriology*. New York: Springer, pp. 473–599.
- Celepli, N., Sundh, J., Ekman, M., Dupont, C.L., Yooseph, S., Bergman, B. et al. (2017) Meta-omic analyses of Baltic Sea cyanobacteria: diversity, community structure and salt acclimation. *Environmental Microbiology*, 19, 673–686.
- Chen, F., Wang, K., Kan, J., Suzuki, M.T. & Wommack, K.E. (2006) Diverse and unique picocyanobacteria in Chesapeake Bay, revealed by 16S-23S rRNA internal transcribed spacer sequences. *Applied and Environmental Microbiology*, 72, 2239–2243.
- Crosbie, N.D., Pöckl, M. & Weisse, T. (2003) Dispersal and phylogenetic diversity of nonmarine picocyanobacteria, inferred from 16S rRNA gene and *cpcBA*-intergenic spacer sequence analyses. *Applied and Environmental Microbiology*, 69, 5716–5721.
- Cruz, B.N. & Neuer, S. (2019) Heterotrophic bacteria enhance the aggregation of the marine picocyanobacteria *Prochlorococcus* and *Synechococcus*. *Frontiers in Microbiology*, 10, 1864.
- Di Cesare, A., Cabello-Yeves, P.J., Christmas, N.A.M., Sánchez-Baracaldo, P., Salcher, M.M. & Callieri, C. (2018) Genome analysis of the freshwater planktonic *Vulcanococcus limneticus* sp. nov. reveals horizontal transfer of nitrogenase operon and alternative pathways of nitrogen utilization. *BMC Genomics*, 19, 259.
- Di Cesare, A., Dzhenbekova, N., Cabello-Yeves, P.J., Eckert, E.M., Slabakova, V., Slabakova, N. et al. (2020) Genomic comparison and spatial distribution of different *Synechococcus* phylotypes in the Baltic Sea. *Frontiers in Microbiology*, 11, 1979.
- Doré, H., Farrant, G.K., Guyet, U., Haguait, J., Humily, F., Ratn, M. et al. (2020) Evolutionary mechanisms of long-term genome



- diversification associated with niche partitioning in marine picocyanobacteria. *Frontiers in Microbiology*, 11, 567431.
- Dufresne, A., Ostrowski, M., Scanlan, D.J., Garczarek, L., Mazard, S., Palenik, B.P. et al. (2008) Unraveling the genomic mosaic of a ubiquitous genus of marine cyanobacteria. *Genome Biology*, 9, R90.
- Ernst, A., Becker, S., Wollenzien, U.I.A. & Postius, C. (2003) Ecosystem-dependent adaptive radiations of picocyanobacteria inferred from 16S rRNA and ITS-1 sequence analysis. *Microbiology*, 149, 217–228.
- Farrant, G.K., Doré, H., Cornejo-Castillo, F.M., Partensky, F., Ratin, M., Ostrowski, M. et al. (2016) Delineating ecologically significant taxonomic units from global patterns of marine picocyanobacteria. *Proceedings of the National Academy of Sciences*, 113, E3365–E3374.
- Ferrieux, M., Dufour, L., Doré, H., Ratin, M., Guéneuguès, A., Chasselin, L. et al. (2022) Comparative thermophysiology of marine *Synechococcus* CRD1 strains isolated from different thermal niches in iron-depleted areas. *Frontiers in Microbiology*, 13, 893413.
- Flombaum, P., Wang, W.-L., Primeau, F.W. & Martiny, A.C. (2020) Global picophytoplankton niche partitioning predicts overall positive response to ocean warming. *Nature Geoscience*, 13, 116–120.
- Fucich, D., Marsan, D., Sosa, A. & Chen, F. (2019) Complete genome sequence of subcluster 5.2 *Synechococcus* sp. strain CB0101, isolated from the Chesapeake Bay. *Microbiology Resource Announcements*, 8, e00484–e00419.
- Fucich, D., Xu, Y., Sosa, A., Jia, Y., Zhang, R., Jiao, N. et al. (2021) Complete genome sequences of Chesapeake Bay *Synechococcus* strains CBW1002 and CBW1006 isolated in winter. *Genome Biology and Evolution*, 13, evab009.
- Gargas, E. (1975) *A manual for phytoplankton primary production studies in the Baltic*. Baltic Marine Biologists. Publ. No. 2. Hørsholm, Denmark: Water Quality Institute.
- Goericke, R. & Montoya, J.P. (1998) Estimating the contribution of microalgal taxa to chlorophyll a in the field—variations of pigment ratios under nutrient- and light-limited growth. *Marine Ecology Progress Series*, 169, 97–112.
- Grébert, T., Doré, H., Partensky, F., Farrant, G.K., Boss, E.S., Picheral, M. et al. (2018) Light color acclimation is a key process in the global ocean distribution of *Synechococcus* cyanobacteria. *Proceedings of the National Academy of Sciences*, 115, E2010–E2019.
- Guillard, R.R.L., & Hargraves, P.E. (1993) *Stichochrysis immobilis* is a diatom, not a chrysophyte. *Phycologia*, 32, 234–236.
- Haverkamp, T., Acinas, S.G., Doeleman, M., Stomp, M., Huisman, J. & Stal, L.J. (2008) Diversity and phylogeny of Baltic Sea picocyanobacteria inferred from their ITS and phycobiliprotein operons. *Environmental Microbiology*, 10, 174–188.
- Haverkamp, T.H.A., Schouten, D., Doeleman, M., Wollenzien, U., Huisman, J. & Stal, L.J. (2009) Colorful microdiversity of *Synechococcus* strains (picocyanobacteria) isolated from the Baltic Sea. *The ISME Journal*, 3, 397–408.
- HELCOM. (2021) Climate change in the Baltic Sea. 2021 fact sheet. Baltic Sea environment proceedings n°180. HELCOM/Baltic earth 2021.
- Hoang, D.T., Chernomor, O., von Haeseler, A., Minh, B.Q. & Vinh, L. S. (2018) UFBoot2: improving the ultrafast bootstrap approximation. *Molecular Biology and Evolution*, 35, 518–522.
- Honda, D., Yokota, A. & Sugiyama, J. (1999) Detection of seven major evolutionary lineages in cyanobacteria based on the 16S rRNA gene sequence analysis with new sequences of five marine *Synechococcus* strains. *Journal of Molecular Evolution*, 48, 723–739.
- Hu, Y.O.O., Karlson, B., Charvet, S. & Andersson, A.F. (2016) Diversity of pico- to mesoplankton along the 2000 km salinity gradient of the Baltic Sea. *Frontiers in Microbiology*, 7, 679.
- Huber, P., Cornejo-Castillo, F.M., Ferrera, I., Sánchez, P., Logares, R., Metz, S. et al. (2019) Primer design for an accurate view of picocyanobacterial community structure by using high-throughput sequencing. *Applied and Environmental Microbiology*, 85, e02659–e02618.
- Hugerth, L.W., Larsson, J., Alneberg, J., Lindh, M.V., Legrand, C., Pinhassi, J. et al. (2015) Metagenome-assembled genomes uncover a global brackish microbiome. *Genome Biology*, 16, 279.
- Hunter-Cevera, K.R., Neubert, M.G., Olson, R.J., Solow, A.R., Shalapyonok, A. & Sosik, H.M. (2016) Physiological and ecological drivers of early spring blooms of a coastal phytoplankton. *Science*, 354, 326–329.
- Jeffrey, S.W. & Humphrey, G.F. (1975) New spectrophotometric equations for determining chlorophylls a, b, c1 and c2 in higher plants, algae and natural phytoplankton. *Biochimie und Physiologie der Pflanzen*, 167, 191–194.
- Jiang, Y., Xiong, X., Danska, J. & Parkinson, J. (2016) Metatranscriptomic analysis of diverse microbial communities reveals core metabolic pathways and microbiome-specific functionality. *Microbiome*, 4, 2.
- Johnson, Z.I. & Sheldon, T.L. (2007) A high-throughput method to measure photosynthesis-irradiance curves of phytoplankton. *Limnology and Oceanography: Methods*, 5, 417–424.
- Kalyaanamoorthy, S., Minh, B.Q., Wong, T.K.F., von Haeseler, A. & Jermin, L.S. (2017) ModelFinder: fast model selection for accurate phylogenetic estimates. *Nature Methods*, 14, 587–589.
- Katoh, K., Rozewicki, J. & Yamada, K.D. (2019) MAFFT online service: multiple sequence alignment, interactive sequence choice and visualization. *Briefings in Bioinformatics*, 20, 1160–1166.
- Kulk, G., de Vries, P., van de Poll, W.H., Visser, R.J.W. & Buma, A.G. J. (2012) Temperature-dependent growth and photophysiology of prokaryotic and eukaryotic oceanic picophytoplankton. *Marine Ecology Progress Series*, 466, 43–55.
- Lane, D. (1991) 16S/23S rRNA sequencing. In: Stackebrandt, E. & Goodfellow, M. (Eds.) *Nucleic acid techniques in bacterial systematics*. New York: John Wiley and Sons, pp. 115–175.
- Larsson, J., Celepli, N., Ininbergs, K., Dupont, C.L., Yooseph, S., Bergman, B. et al. (2014) Picocyanobacteria containing a novel pigment gene cluster dominate the brackish water Baltic Sea. *The ISME Journal*, 8, 1892–1903.
- Liu, H., Jing, H., Wong, T.H.C. & Chen, B. (2014) Co-occurrence of phycocyanin- and phycoerythrin-rich *Synechococcus* in subtropical estuarine and coastal waters of Hong Kong. *Environmental Microbiology Reports*, 6, 90–99.
- Mackey, K.R.M., Post, A.F., McIlvin, M.R. & Saito, M.A. (2017) Physiological and proteomic characterization of light adaptations in marine *Synechococcus*. *Environmental Microbiology*, 19, 2348–2365.
- Marsan, D., Wommack, K.E., Ravel, J. & Chen, F. (2014) Draft genome sequence of *Synechococcus* sp. strain CB0101, isolated from the Chesapeake Bay estuary. *Genome Announcements*, 2, e01111–e01113.
- Masamoto, K. & Furukawa, K. (1997) Accumulation of zeaxanthin in cells of the cyanobacterium, *Synechococcus* sp. strain PCC 7942 grown under high irradiance. *Journal of Plant Physiology*, 151, 257–261.
- Minh, B.Q., Schmidt, H.A., Chernomor, O., Schrempf, D., Woodhams, M.D., von Haeseler, A. et al. (2020) IQ-TREE 2: new models and efficient methods for phylogenetic inference in the genomic era. *Molecular Biology and Evolution*, 37, 1530–1534.
- Ospina-Serna, J., Huber, P., Odriozola, M., Fermani, P. & Unrein, F. (2020) Picocyanobacteria aggregation as a response to predation pressure: direct contact is not necessary. *FEMS Microbiology Ecology*, 96, fiae153.
- Paerl, R.W., Venezia, R.E., Sanchez, J.J. & Paerl, H.W. (2020) Picophytoplankton dynamics in a large temperate estuary and impacts of extreme storm events. *Scientific Reports*, 10, 22026.

- Partensky, F., Blanchot, J. & Vaulot, D. (1999) Differential distribution and ecology of *Prochlorococcus* and *Synechococcus* in oceanic waters: a review. *Bulletin de l'Institut océanographique*, 19, 457–476.
- Pittera, J., Humily, F., Thorel, M., Grulois, D., Garczarek, L. & Six, C. (2014) Connecting thermal physiology and latitudinal niche partitioning in marine *Synechococcus*. *The ISME Journal*, 8, 1221–1236.
- Platt, T., Gallegos, C.L. & Harrison, W.G. (1980) Photoinhibition of photosynthesis in natural assemblages of marine phytoplankton. *Journal of Marine Research*, 38, 687–701.
- R Core Team. (2022) *R: a language and environment for statistical computing*. Vienna, Austria: R foundation for statistical computing. <https://www.R-project.org/>
- Richardson, K., Beardall, J. & Raven, J.A. (1983) Adaptation of unicellular algae to irradiance: an analysis of strategies. *The New Phytologist*, 93, 157–191.
- Salazar, V.W., Tschoeke, D.A., Swings, J., Cosenza, C.A., Mattoso, M., Thompson, C.C. et al. (2020) A new genomic taxonomy system for the *Synechococcus* collective. *Environmental Microbiology*, 22, 4557–4570.
- Sánchez-Baracaldo, P., Bianchini, G., Di Cesare, A., Callieri, C. & Chrismas, N.A.M. (2019) Insights into the evolution of picocyanobacteria and phycoerythrin genes (mpeBA and cpeBA). *Frontiers in Microbiology*, 10, 45.
- Sánchez-Baracaldo, P., Handley, B.A. & Hayes, P.K. (2008) Picocyanobacterial community structure of freshwater lakes and the Baltic Sea revealed by phylogenetic analyses and clade-specific quantitative PCR. *Microbiology*, 154, 3347–3357.
- Scanlan, D.J., Ostrowski, M., Mazard, S., Dufresne, A., Garczarek, L., Hess, W.R. et al. (2009) Ecological genomics of marine picocyanobacteria. *Microbiology*, 73, 249–299.
- Schallenberg, L.A., Wood, S.A., Puddick, J., Cabello-Yeves, P.J. & Burns, C.W. (2022) Isolation and characterisation of monoclonal picocyanobacterial strains from contrasting New Zealand lakes. *Inland Waters*, 12, 383–396.
- Seemann, T. (2014) Prokka: rapid prokaryotic genome annotation. *Bioinformatics*, 30, 2068–2069.
- Six, C., Ratin, M., Marie, D. & Corre, E. (2021) Marine *Synechococcus* picocyanobacteria: light utilization across latitudes. *Proceedings of the National Academy of Sciences*, 118, e2111300118.
- Six, C., Thomas, J.-C., Garczarek, L., Ostrowski, M., Dufresne, A., Blot, N. et al. (2007) Diversity and evolution of phycobilisomes in marine *Synechococcus* spp.: a comparative genomics study. *Genome Biology*, 8, R259.
- Śliwińska-Wilczewska, S., Cieszyńska, A., Maculewicz, J. & Latała, A. (2018) Ecophysiological characteristics of red, green, and brown strains of the Baltic picocyanobacterium *Synechococcus* sp.—a laboratory study. *Biogeosciences*, 15, 6257–6276.
- Śliwińska-Wilczewska, S., Konarzewska, Z., Wiśniewska, K. & Konik, M. (2020) Photosynthetic pigments changes of three phenotypes of picocyanobacteria *Synechococcus* sp. under different light and temperature conditions. *Cell*, 9, E2030.
- Sohm, J.A., Ahlgren, N.A., Thomson, Z.J., Williams, C., Moffett, J.W., Saito, M.A. et al. (2016) Co-occurring *Synechococcus* ecotypes occupy four major oceanic regimes defined by temperature, macronutrients and iron. *The ISME Journal*, 10, 333–345.
- Stawiarski, B., Buitenhuis, E.T. & Le Quééré, C. (2016) The physiological response of picophytoplankton to temperature and its model representation. *Frontiers in Marine Science*, 3, 164.
- Stecher, G., Tamura, K. & Kumar, S. (2020) Molecular evolutionary genetics analysis (MEGA) for macOS. *Molecular Biology and Evolution*, 37, 1237–1239.
- Stomp, M., Huisman, J., de Jongh, F., Veraart, A.J., Gerla, D., Rijkeboer, M. et al. (2004) Adaptive divergence in pigment composition promotes phytoplankton biodiversity. *Nature*, 432, 104–107.
- Stomp, M., Huisman, J., Vörös, L., Pick, F.R., Laamanen, M., Haverkamp, T. et al. (2007) Colourful coexistence of red and green picocyanobacteria in lakes and seas. *Ecology Letters*, 10, 290–298.
- Strickland, J.D.H. & Parsons, T.R. (1968) A practical handbook of seawater analysis. *Canadian Journal of Fisheries and Aquatic Sciences*, 167, 1–310.
- Takaichi, S. & Mochimaru, M. (2007) Carotenoids and carotenogenesis in cyanobacteria: unique ketocarotenoids and carotenoid glycosides. *Cellular and Molecular Life Sciences*, 64, 2607–2619.
- Visintini, N., Martiny, A.C. & Flombaum, P. (2021) *Prochlorococcus*, *Synechococcus*, and picoeukaryotic phytoplankton abundances in the global ocean. *Limnology and Oceanography Letters*, 6, 207–215.
- Wang, K., Wommack, K.E. & Chen, F. (2011) Abundance and distribution of *Synechococcus* spp. and cyanophages in the Chesapeake Bay. *Applied and Environmental Microbiology*, 77, 7459–7468.
- Wollschläger, J., Neale, P.J., North, R.L., Striebel, M. & Zielinski, O. (2021) Editorial: climate change and light in aquatic ecosystems: variability & ecological consequences. *Frontiers in Marine Science*, 8, 688712.
- Xia, X., Guo, W., Tan, S. & Liu, H. (2017) *Synechococcus* assemblages across the salinity gradient in a salt wedge estuary. *Frontiers in Microbiology*, 8, 1254.
- Xia, X., Vidyarthna, N.K., Palenik, B., Lee, P. & Liu, H. (2015) Comparison of the seasonal variations of *Synechococcus* assemblage structures in estuarine waters and coastal waters of Hong Kong. *Applied and Environmental Microbiology*, 81, 7644–7655.
- Xu, Y., Jiao, N. & Chen, F. (2015) Novel psychrotolerant picocyanobacteria isolated from Chesapeake Bay in the winter. *Journal of Phycology*, 51, 782–790.

## SUPPORTING INFORMATION

Additional supporting information can be found online in the Supporting Information section at the end of this article.

**How to cite this article:** Aguilera, A., Alegria Zúfia, J., Bas Conn, L., Gurlit, L., Śliwińska-Wilczewska, S., Budzałek, G. et al. (2023) Ecophysiological analysis reveals distinct environmental preferences in closely related Baltic Sea picocyanobacteria. *Environmental Microbiology*, 1–22. Available from: <https://doi.org/10.1111/1462-2920.16384>